

Fast, Stable and Efficient Approximation of Multi-parameter Persistence Modules with MMA

David Loiseaux, Mathieu Carrière, Andrew J. Blumberg

June 21, 2023

Abstract

Topological data analysis (TDA) is a rapidly growing area of data science which uses the geometry and topology of data sets to produce qualitative multi-scale shape descriptors for subsequent statistical and machine learning tasks. The most common descriptor in TDA is persistent homology, which tracks the topological changes in growing families of subsets of the data set itself, called filtrations, and encodes them in an algebraic object, called a persistence module. The algorithmic and theoretical properties of persistence modules are now well understood in the single-parameter case, that is, when there is only one filtration (e.g., feature scale) to study. In contrast, much less is known in the multi-parameter case, where several filtrations (e.g., scale and density) are used simultaneously. Indeed, the resulting multi-parameter persistence modules are much more complicated and intricate, which dramatically impedes the study of their theoretical properties. However, they usually encode information that is invisible to their single-parameter counterparts, and are thus much more useful descriptors for applications in data science. As a consequence, a lot of attention has been devoted to the construction of tractable and stable proxies for multi-parameter persistence modules. However, most of the proposed approaches in the literature are still prohibitively expensive to compute on large-scale data, many are limited to at most two filtrations, and the most tractable sacrifice much of the richness of the multi-parameter setting.

In this article, we introduce a new parameterized family of topological invariants, taking the form of candidate decompositions, for multi-parameter persistence modules. We prove that our candidate decompositions are controllable approximations: when restricting to modules that can be decomposed into interval summands, we establish theoretical results about the approximation error between our candidate decompositions and the true underlying module in terms of the standard interleaving and bottleneck distances. Moreover, even when the underlying module does not admit such a decomposition, our candidate decompositions are nonetheless stable invariants; small perturbations in the underlying module lead to small perturbations in the candidate decomposition. Then, we introduce **MMA** (Multipersistence Module Approximation): an algorithm for computing stable instances of such invariants, which is based on fibered barcodes and exact matchings, two constructions that stem from the theory of single-parameter persistence. By design, **MMA** can handle an arbitrary number of filtrations, and has bounded complexity and running time. Finally, we present empirical evidence validating the generalization capabilities and running time speed-ups of **MMA** on several data sets.

1 Introduction

Topological Data Analysis (TDA) [EH10, Oud15] is a new and rapidly developing area of data science that has seen a lot of interest due to its success in various applications, ranging from bioinformatics [RB19] to material science [BHO18]. The main computational tool of TDA is *persistent homology* (PH). Whereas homology is a qualitative descriptor of the shape of a topological space S^1 , the core idea of PH is to capture how the homology groups change when computed on a *filtration* of S . A filtration is a family $\{S_x \subseteq S\}_{x \in \mathcal{A}}$ of subspaces of S indexed over a partially ordered set (poset) \mathcal{A} , that is *nested w.r.t. inclusion*, i.e., it satisfies $S_x \subseteq S_y$ for any $x \leq y$. Then, the functoriality of homology and these inclusions induce morphisms between the corresponding

¹In this article, we work with simplicial homology, hence it is assumed throughout the article that S is a *simplicial complex*.

homology groups $H_*(S_x) \rightarrow H_*(S_y)$ for each pair $x \leq y$, which allows to detect the differences in homology when going from index x to index y . One of the most common ways to produce such filtrations is to study the *sublevel sets* of a continuous *filter* function $f : S \rightarrow \mathbb{R}^n$, defined with $S_x = f^{-1}(\{x' \in \mathbb{R}^n : x' \leq_n x\})$; the partial order on the poset \mathbb{R}^n (denoted by \leq_n) is defined, for $x, y \in \mathbb{R}^n$, as $x \leq_n y$ if and only if $x_i \leq y_i$ for every dimension i .

Single-parameter PH. When \mathcal{A} is totally ordered, e.g., when $\mathcal{A} \subseteq \mathbb{R}$, then applying the homology functor $H_*(-; k)$ for a field k to a (single-parameter) filtration results in a sequence of vector spaces connected by linear maps, called a *single-parameter persistence module*. This situation has been studied extensively in the TDA literature [Car09, CdSGO16, EH10, Oud15]. Notably, one can show that such persistence modules can always be decomposed into a direct sum of simple *interval summands*: $\mathbb{M} \simeq \bigoplus_{i \in \mathcal{I}} I(b_i, d_i)$, where each interval summand $I(b_i, d_i)$ intuitively represents the lifetime of a topological structure, i.e., b_i is the appearance time (birth) and d_i is the disappearance time (death) of a topological structure, that is detected by homology as the index increases. Moreover, single-parameter persistence modules can be efficiently represented in a compact descriptor called the *persistence barcode*, and several representation methods, such as Euclidean embeddings and kernels for machine learning classifiers, have been proposed for such barcodes in the literature [Bub15, AEK⁺17, RHBK15, CCO17, CCI⁺20]. As a consequence, most applications of TDA use single-parameter persistence modules, and often use the sublevel sets of, e.g., the data set scale, as the corresponding single-parameter filtration.

Multi-parameter PH. However, many data sets come with not just one, but multiple, possibly intertwined, salient filtrations. For example, image data typically has both a spatial filtration and an intensity filtration, and arbitrary point cloud data can be filtered both by feature scale and density. Unfortunately, in general, the resulting *multi-parameter persistence modules*, obtained by applying the homology functor to a filtration indexed over \mathbb{R}^n [BL22], are much less tractable; in contrast to the single-parameter case, there is no decomposition theorem that can break down any module into a direct sum of simple indicator summands (e.g., interval modules). Instead, there is now a rich literature on general decompositions into arbitrarily complicated summands [DX22] and their associated minimal presentations [KR21, LW19], and on the theoretical study of a few restricted cases (such as $n = 2$ filtrations or multi-parameter persistence modules in homology dimension 0) where simple decompositions can be obtained [ABE⁺18, AENY19, BLOry, CO19, DX21]. It has thus become crucial to define general topological invariants for multi-parameter persistence modules that are meaningful, visually interpretable, and easily computable.

Contributions. In this article, we introduce new invariants of multi-parameter persistence modules (obtained from the persistent homology of multi-parameter filtrations of simplicial complexes), along with a new algorithm we call **MMA** for their practical computations. More precisely, our contributions are five-fold:

1. We introduce a new family of topological invariants for multi-parameter persistence modules (Definition 3.3), taking the form of *candidate decompositions* $\tilde{\mathbb{M}}_\delta = \bigoplus_{i \in \tilde{\mathcal{I}}} \tilde{I}_i$. These candidate decompositions are parameterized by a precision parameter $\delta > 0$, and each \tilde{I}_i in these candidate decompositions is an interval summand in \mathbb{R}^n .
2. When computed over *interval decomposable* modules, we prove that under mild assumptions the interleaving and bottleneck distances between our candidate decompositions $\tilde{\mathbb{M}}_\delta$ and the module \mathbb{M} they approximate are upper bounded (Proposition 3.4):

$$d_1(\mathbb{M}, \tilde{\mathbb{M}}_\delta) \leq d_B(\mathbb{M}, \tilde{\mathbb{M}}_\delta) \leq \delta.$$

3. We introduce our method **MMA** (Multi-parameter persistence Module Approximation, Algorithm 1) for computing instances of such candidate decompositions, with running time

$$O\left(N^3 + \frac{1}{\delta^{n-1}}(N + n \cdot 2^{n-1})\right),$$

where N is the number of simplices and n is the number of filtrations. See Figure 1. Note that MMA does not require the input module \mathbb{M} to be interval decomposable in order to run.

4. We study the approximation and stability properties of MMA. More precisely, we show that when δ becomes small enough, the candidate decompositions $\tilde{\mathbb{M}}_\delta^{\text{MMA}}$ computed by MMA recover the underlying persistence module \mathbb{M} exactly, provided that it is interval decomposable (Corollary 4.10):

$$d_I(\mathbb{M}, \tilde{\mathbb{M}}_\delta^{\text{MMA}}) = d_B(\mathbb{M}, \tilde{\mathbb{M}}_\delta^{\text{MMA}}) = 0,$$

when δ is less than a constant that depends only on the multi-parameter filtration values. In the general case (when \mathbb{M} is not necessarily interval decomposable), we show that the candidate decompositions produced by MMA preserve the (single-parameter) persistence barcodes associated to diagonal slices of the multi-parameter filtration (Proposition 4.12):

$$d_B(\mathcal{B}(\mathbb{M}|_l), \mathcal{B}(\tilde{\mathbb{M}}_\delta^{\text{MMA}}|_l)) \leq 2\delta,$$

and that they are also stable w.r.t. the input data (Proposition 4.13):

$$d_I(\tilde{\mathbb{M}}_\delta^{\text{MMA}}(f), \tilde{\mathbb{M}}_\delta^{\text{MMA}}(g)) \leq d_B(\tilde{\mathbb{M}}_\delta^{\text{MMA}}(f), \tilde{\mathbb{M}}_\delta^{\text{MMA}}(g)) \leq \|f - g\|_\infty + \delta,$$

where $\tilde{\mathbb{M}}_\delta^{\text{MMA}}(f)$ stands for the candidate decomposition that is induced by the sublevel sets of f and computed with MMA (and similarly for g).

5. We discuss practical choices of the input parameters of MMA in Section 5, and we perform numerical experiments that showcase the performance of MMA and exhibit the trade-off between computation time and approximation error in Section 6.

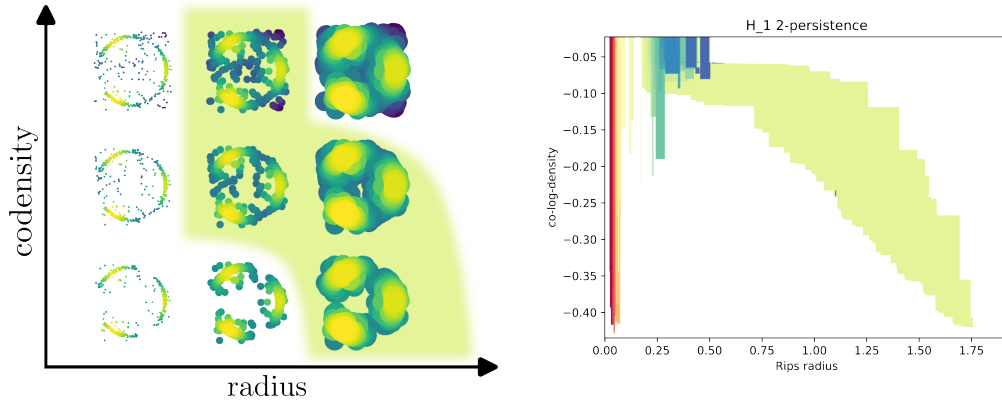


Figure 1: Example of candidate decomposition computed by MMA on a point cloud filtered by both growing balls around the points (also called *Čech filtration*) and using the sublevel sets of codensity (or, equivalently, the superlevel sets of density), in homology dimension 1. One can see that there is a large lightgreen summand in the candidate decomposition on the right that corresponds to the cycle formed by the points amid outliers, which is also highlighted in lightgreen in the multi-parameter filtration on the left.

An important input parameter of our method MMA is the so-called *matching function* σ , which has a large influence on the candidate decompositions produced by MMA. While the output of MMA is only an approximation of the underlying module \mathbb{M} , we hypothesize that, in the general case, the family \mathcal{F} of candidate decompositions obtained from MMA by varying the matching function parameter across an appropriate family of matching functions Σ , as $\mathcal{F} = \{\text{MMA}(\mathbb{M}, L_\delta, \sigma)\}_{\sigma \in \Sigma, \delta > 0}$, is a complete invariant of the underlying module \mathbb{M} . We leave this conjecture open for future work.

Related work. The most common topological invariants of multi-parameter persistence modules are the so-called *Hilbert function* HF and *rank invariant* RI. The Hilbert function simply gathers the dimensions of all vector spaces in the module $\text{HF} = x \mapsto \dim(H_*(S_x))$, i.e., it counts the number of topological structures that are present in S_x at index x , while the rank invariant gathers the ranks of all morphisms in the module $\text{RI} = (x, y) \mapsto \text{rank}(H_*(S_x) \rightarrow H_*(S_y))$ (if $x \leq_n y$), i.e., it counts the topological structures that are preserved when going from index x to index y . The rank invariant is equivalent to computing the persistence barcodes associated to all possible lines in \mathbb{R}^n ; this slicing process is usually referred to as the *fibred barcode*. The Hilbert function, the rank invariant and the fibred barcode can all be computed with the **Rivet** software [LW15] in $O(N^3\kappa + (N + \log\kappa)\kappa^2)$ operations, where N is the number of simplices, and κ is the number of indices on which HF and RI are evaluated. Note that Hilbert functions and rank invariants can also be decomposed themselves in order to be more visually interpretable—the corresponding invariants are called *signed barcodes* [BOO21].

Unfortunately, **Rivet** is currently limited to at most $n = 2$ filtrations. Moreover, invariants based on dimensions and ranks are known to miss a lot of the structural properties of modules: it is quite easy to find examples of distinct modules that share the same Hilbert function and rank invariant [Vip20a, Figure 3]. Thus, generalizations of the Hilbert function, the rank invariant, the signed barcodes, and their corresponding algorithms, have been introduced recently [DKM22, KM18]. To our knowledge, there is however no corresponding available implementations of these tools.

Finally, another recent line of work also provides candidate decompositions into simple summands for modules that are computed from point cloud data. These decompositions are obtained from applying the elder rule and called the *elder-rule staircodes* [CKMW20], with running time $O(m^2 \log(m))$ where m is the number of points of the point cloud. This approach has been shown to be theoretically close to the true decomposition, but only works in homology dimension 0 and for $n = 2$ parameters.

Hence, computing candidate decompositions for multi-parameter persistence modules indexed over \mathbb{R}^n for arbitrary $n \in \mathbb{N}^*$ with controlled complexity, running time, and approximation error is still an open and important question, which we tackle in this article using our approximation scheme **MMA**.

Outline. Section 2 provides a concise review of multi-parameter persistence modules. In Section 3, we present our new invariants for multi-parameter persistence modules and their approximation properties. Then, we introduce our corresponding algorithm **MMA** and its stability properties in Section 4. We also discuss the choice of its input parameters in Section 5. Finally, we illustrate the performances of **MMA** in Section 6.

2 Background

In this section, we recall the basics of multi-parameter persistence modules. This section only contains the necessary background and notations, and can be skipped if the reader is already familiar with persistence theory. A more complete treatment of persistence modules can be found in [CdSGO16, DW22, Oud15].

Multi-parameter persistence modules. In their most general form, multi-parameter persistence modules are nothing but k -vector spaces (where k denotes a field) indexed by \mathbb{R}^n and connected by linear maps.

Definition 2.1 (Multi-parameter persistence module). *An (n) -multi-parameter persistence module \mathbb{M} is a family of vector spaces indexed over \mathbb{R}^n : $\mathbb{M} = \{M_x\}_{x \in \mathbb{R}^n}$, equipped with linear transformations $\{\varphi_x^y : M_x \rightarrow M_y\}_{x, y \in \mathbb{R}^n, x \leq_n y}$, that are called the transition maps of \mathbb{M} , and that satisfy $\varphi_x^z = \varphi_y^z \circ \varphi_x^y$ for any $x \leq_n y \leq_n z$.*

A morphism between two multi-parameter persistence modules \mathbb{M}, \mathbb{M}' with transition maps φ and ψ , respectively, is a collection of linear maps $f = \{f_x : M_x \rightarrow M'_x\}_{x \in \mathbb{R}^n}$, that commutes with transitions maps, i.e., one has $f_y \circ \varphi_x^y = \psi_x^y \circ f_x$, for all $x \leq_n y$.

In this article, all multi-parameter persistence modules come from applying the *homology functor* H_* on a *multi-parameter filtration* of a simplicial complex S , that is, on a family $\{S_x\}_{x \in \mathbb{R}^n}$ of subsets of S indexed over \mathbb{R}^n such that $x \leq_n y \Rightarrow S_x \subseteq S_y$. In other words, we study modules of the form $\mathbb{M} := \{H_*(S_x)\}_{x \in \mathbb{R}^n}$,

where the linear maps $H_*(S_x) \rightarrow H_*(S_y)$ are induced by the canonical inclusions $S_x \subseteq S_y$ (when $x \leq_n y$). There are many interesting multi-parameter filtrations in data science; one of the most common one (with $n = 2$) comes from filtering by feature scale and density. This allows to detect the topological structures (encoded in the homology groups) of point clouds in the face of noise and outliers [BL20, CB20].

Definition 2.2. *The direct sum of two multi-parameter persistence modules \mathbb{M} and \mathbb{M}' , written as $\mathbb{M} \oplus \mathbb{M}'$, is the module \mathbb{M}'' with vector spaces $\{M''_x\}_{x \in \mathbb{R}^n}$ and transition maps (ϕ'') , defined as $M''_x = M_x \oplus M'_x$ for all $x \in \mathbb{R}^n$, and $(\phi'') = \phi \oplus (\phi')$, where $\{M_x\}_{x \in \mathbb{R}^n}$ (resp. $\{M'_x\}_{x \in \mathbb{R}^n}$) and ϕ (resp. (ϕ')) are the vector spaces and transition maps of \mathbb{M} (resp. \mathbb{M}') respectively.*

A multi-parameter persistence module \mathbb{M} such that there are no modules A and B such that $\mathbb{M} \simeq A \oplus B$ is called indecomposable.

Note that while multi-parameter persistence modules can always be decomposed into indecomposable summands (see [DX22] for a corresponding algorithm), these summands can be arbitrarily complicated, and the resulting decomposition cannot really be used as an intuitive and simple invariant of the module.

Distances between modules. Multi-parameter persistence modules can be compared with the standard interleaving distance [Les15].

Definition 2.3 (Interleaving distance). *Given $\varepsilon > 0$, two multi-parameter persistence modules \mathbb{M} and \mathbb{M}' are ε -interleaved if there exist two morphisms $f: \mathbb{M} \rightarrow \mathbb{M}'(\varepsilon)$ and $g: \mathbb{M}' \rightarrow \mathbb{M}(\varepsilon)$ such that $g_{+\varepsilon} \circ f = \varphi_{+2\varepsilon}$ and $f_{+\varepsilon} \circ g = \psi_{+2\varepsilon}$, where $\mathbb{M}(\varepsilon)$ is the shifted module $\{M_{x+\varepsilon}\}_{x \in \mathbb{R}^n}$, $\varepsilon = (\varepsilon, \dots, \varepsilon) \in \mathbb{R}^n$, and φ and ψ are the transition maps of \mathbb{M} and \mathbb{M}' respectively.*

The interleaving distance between two multi-parameter persistence modules \mathbb{M} and \mathbb{M}' is then defined as $d_I(\mathbb{M}, \mathbb{M}') := \inf \{\varepsilon \geq 0 : \mathbb{M} \text{ and } \mathbb{M}' \text{ are } \varepsilon\text{-interleaved}\}$.

The main property of this distance is that it is *stable* for multi-parameter filtrations that are obtained from the sublevel sets of functions. More precisely, given two continuous functions $f, g: S \rightarrow \mathbb{R}^n$ defined on a simplicial complex S , and such that $\tau \subseteq \sigma \Rightarrow f(\tau) \leq_n f(\sigma)$ for any $\tau, \sigma \in S$ (and similarly for g), let $\mathbb{M}(f), \mathbb{M}(g)$ denote the multi-parameter persistence modules obtained from the corresponding multi-parameter filtrations $\{S_x^f := \{\sigma \in S : f(\sigma) \leq_n x\}\}_{x \in \mathbb{R}^n}$ and $\{S_x^g := \{\sigma \in S : g(\sigma) \leq_n x\}\}_{x \in \mathbb{R}^n}$. Then, one has [Les15, Theorem 5.3]:

$$d_I(\mathbb{M}(f), \mathbb{M}(g)) \leq \|f - g\|_\infty. \quad (1)$$

Another usual distance is the *bottleneck distance* [BL18, Section 2.3]. Intuitively, it relies on decompositions of the modules into direct sums of indecomposable summands, and is defined as the largest interleaving distance between summands that are matched under some matching.

Definition 2.4 (Bottleneck distance). *Given two multisets A and B , $\mu: A \dashrightarrow B$ is called a matching if there exist $A' \subseteq A$ and $B' \subseteq B$ such that $\mu: A' \rightarrow B'$ is a bijection. The subset $A' := \text{coim}(\mu)$ (resp. $B' := \text{im}(\mu)$) is called the coimage (resp. image) of μ .*

Let $\mathbb{M} \cong \bigoplus_{i \in \mathcal{I}} M_i$ and $\mathbb{M}' \cong \bigoplus_{j \in \mathcal{J}} M'_j$ be two multi-parameter persistence modules. Given $\varepsilon \geq 0$, the modules \mathbb{M} and \mathbb{M}' are ε -matched if there exists a matching $\mu: \mathcal{I} \dashrightarrow \mathcal{J}$ such that M_i and $M'_{\mu(i)}$ are ε -interleaved for all $i \in \text{coim}(\mu)$, and M_i (resp. M'_j) is ε -interleaved with the null module $\mathbf{0}$ for all $i \in \mathcal{I} \setminus \text{coim}(\mu)$ (resp. $j \in \mathcal{J} \setminus \text{im}(\mu)$).

The bottleneck distance between two multi-parameter persistence modules \mathbb{M} and \mathbb{M}' is then defined as $d_B(\mathbb{M}, \mathbb{M}') := \inf \{\varepsilon \geq 0 : \mathbb{M} \text{ and } \mathbb{M}' \text{ are } \varepsilon\text{-matched}\}$.

Since a matching between the decompositions of two multi-parameter persistence modules induces an interleaving between the modules themselves, it follows that $d_I \leq d_B$. Note also that d_B can actually be arbitrarily larger than d_I , as showcased in [BL18, Section 9].

Interval modules. Our approximation result presented in Section 4.2 is stated for modules that can be decomposed into so-called *interval modules*. Hence, in this section, we define such interval modules. Intuitively, they are modules that are trivial, except on a subset of \mathbb{R}^n called an *interval*.

Definition 2.5 (Interval). *A subset I of \mathbb{R}^n is called an interval if it satisfies:*

- (convexity) *if $p, q \in I$ and $p \leq_n r \leq_n q$ then $r \in I$, and*
- (connectivity) *if $p, q \in I$, then there exists a finite sequence $r_1, r_2, \dots, r_m \in I$, for some $m \in \mathbb{N}$, such that $p \sim r_1 \sim r_2 \sim \dots \sim r_m \sim q$, where \sim can be either \leq_n or \geq_n .*

Definition 2.6 (Indicator module, Interval module). *A multi-parameter persistence module \mathbb{M} is an indicator module if there exists a set $S \subseteq \mathbb{R}^n$, called the support of \mathbb{M} and denoted by $\text{supp}(\mathbb{M})$, such that:*

$$\forall x \in \mathbb{R}^n, M_x = \begin{cases} k & \text{if } x \in S \\ \mathbf{0} & \text{otherwise} \end{cases} \quad \text{and} \quad \forall x, y \in \mathbb{R}^n, \varphi_x^y = \begin{cases} \text{id}_{k \rightarrow k} & \text{if } x \leq_n y \in S \\ 0 & \text{otherwise} \end{cases}$$

where φ_x^y are the transition maps of \mathbb{M} . If S is an interval, \mathbb{M} is called an interval module.

Finally, we define a specific type of interval modules, those whose support is equal to a union of rectangles. We call these modules *discretely presented*—the stable candidate decompositions computed by our algorithm MMA in Section 4 are actually made up of such modules.

Definition 2.7 (Discretely presented interval module). *An interval module I is discretely presented if its support is a locally finite union of rectangles in $\overline{\mathbb{R}^n}$, and whose boundary is an $(n-1)$ -submanifold of \mathbb{R}^n . More precisely, there exist two locally finite families of points, the birth and death critical points of I , denoted by $C_B(I)$ and $C_D(I)$ respectively, such that:*

$$I := \mathbf{Int} \left(\bigcup_{c \in C_B(I)} \bigcup_{c' \in C_D(I)} R_{c,c'} \right), \quad (2)$$

where $R_{c,c'} := \{x \in \mathbb{R}^n : c \leq_n x \leq_n c'\}$ is the rectangle defined by corners c and c' , and $\mathbf{Int}(S)$ (where S is an interval) denotes the interval module whose support is S .

Note that when only one filtration is given, single-parameter persistence modules always decompose into interval modules: $\mathbb{M} \cong \bigoplus_{i \in \mathcal{I}} \mathbf{Int}([b_i, d_i])$ [CdSGO16, Theorem 2.8]. In that case, they are frequently represented as the collection of the interval supports (in \mathbb{R}) of their summands, also called *persistence barcode* $\mathcal{B}(\mathbb{M}) := \{[b_i, d_i]\}_{i \in \mathcal{I}}$.

Fibered barcode. The *fibered barcode* [LW15] is a centerpiece of our approximation scheme, and is defined, given a multi-parameter persistence module \mathbb{M} , as a map that takes as input a line (or segment) l in \mathbb{R}^n , and outputs the persistence barcode associated to the single-parameter persistence module obtained by restricting \mathbb{M} along l . Hence, in the following, we formalize the intersections between multi-parameter persistence modules and lines in \mathbb{R}^n .

Definition 2.8 (Fibered Barcode). *Let \mathbb{M} be a pointwise finite-dimensional multi-parameter persistence module. Given a discrete family of diagonal lines $L \subseteq \mathcal{L}$ (i.e., lines with direction vector $(1, \dots, 1) \in \mathbb{R}^n$), we let the L -fibered barcode (or fibered barcode for short when L is clear) be the family of barcodes associated to restrictions of the module to lines in L , i.e., $\mathcal{FB}(\mathbb{M})_L = \{\mathcal{B}(\mathbb{M}|_l) : l \in L\}$.*

Remark 2.9. *Recall from single-parameter persistence theory that the support of the restriction of \mathbb{M} to l is a set of bars called persistence barcode: $\mathcal{B}(\mathbb{M}|_l) = \text{supp}(\mathbb{M}|_l) = \{[b_i, d_i]\}_{i \in \mathcal{I}(l)}$, where $\mathcal{I}(l)$ is an index set that depends on \mathbb{M} and l . Moreover, when $\mathbb{M} = \bigoplus_{i \in \mathcal{I}} I_i$ is decomposable into interval modules, there are as many bars in the barcode as there are interval summands intersecting the line $\mathcal{B}(\mathbb{M}|_l) = \{\text{supp}(I_i|_l)\}_{i \in \mathcal{I}}$.*

It is also useful to characterize the fibered barcode with *endpoints* of lines.

Definition 2.10 (Birthpoint, Deathpoint). *Given a point $x \in \mathbb{R}^n$ and an interval module I , we call $b_x^I := \min \{x + \delta : \delta \in \mathbb{R}\}$ (resp. $d_x^I = \max \{x + \delta : \delta \in \mathbb{R}\}$) the birthpoint (resp. deathpoint) associated to x and I , where $\delta = (\delta, \dots, \delta) \in \mathbb{R}^n$.*

Similarly, given a diagonal line $l \subseteq \mathbb{R}^n$, we define the birthpoint (resp. deathpoint) associated to l and I as $b_l^I := b_x^I$ (resp. $d_l^I := d_x^I$) for any $x \in l$. See Figure 2

Remark 2.11. *Using birthpoints and deathpoints, the L -fibered barcode of an interval decomposable multi-parameter persistence module $\mathbb{M} = \bigoplus_{i \in \mathcal{I}} I_i$ is written as:*

$$\mathcal{FB}(\mathbb{M})_L = \{\mathcal{B}(\mathbb{M}|_l) : l \in L\} = \{([b_l^I, d_l^I])_{i \in \mathcal{I}} : l \in L\}. \quad (3)$$

3 Approximate candidate decompositions

In this section, we present our family of topological invariants for multi-parameter persistence modules, defined as candidate decompositions into interval summands, in Section 3.1. We then prove their approximation guarantees in Section 3.2.

3.1 Candidate modules and interval decompositions

In this section, given a multi-parameter persistence module \mathbb{M} , we define a family of good proxies for \mathbb{M} (see Definition 3.3), called *candidate decompositions*. These candidate decompositions are multi-parameter persistence modules that can be decomposed into intervals summands, and approximate \mathbb{M} well when \mathbb{M} is interval decomposable itself, in the sense that $d_I(\mathbb{M}, \tilde{\mathbb{M}})$ and $d_B(\mathbb{M}, \tilde{\mathbb{M}})$ are upper bounded for any candidate decomposition $\tilde{\mathbb{M}}$. Practical computations of instances of such candidate decompositions can be done with our MMA algorithm, that we provide in Section 4.2.

(Exact) matchings and grids of lines. Our candidate decompositions depend on so-called *matching functions* and *δ -grids of lines*, that we now define.

Definition 3.1 ((Exact) matching). *Let \mathbb{M} be a multi-parameter persistence module. Let l, l' be two lines in \mathbb{R}^n . A map σ between the persistence barcodes $\sigma: \mathcal{B}(\mathbb{M}|_l) \rightarrow \mathcal{B}(\mathbb{M}|_{l'}) \cup \{\emptyset\}$ is called an $(\mathbb{M}$ -)matching between l and l' if the restriction of σ to $\sigma^{-1}(\mathcal{B}(\mathbb{M}|_{l'}))$ is injective.*

Furthermore, if \mathbb{M} is interval decomposable, $\mathbb{M} = \bigoplus_{i \in \mathcal{I}} I_i$, we let $\iota_1: \mathcal{B}(\mathbb{M}|_l) \rightarrow \mathcal{I}$ and $\iota_2: \mathcal{B}(\mathbb{M}|_{l'}) \rightarrow \mathcal{I}$ be maps that retrieve the indices of the summands corresponding to the bars in $\mathcal{B}(\mathbb{M}|_l)$ and $\mathcal{B}(\mathbb{M}|_{l'})$ as per Equation (3). Then, σ is said to be exact if $\iota_1(b) = \iota_2(\sigma(b))$ for any bar $b \in \sigma^{-1}(\mathcal{B}(\mathbb{M}|_{l'}))$. In other words, bars that are matched under σ correspond to the same underlying interval summand of \mathbb{M} . Note that the interval decomposition of \mathbb{M} always induces a canonical exact matching, that we denote $\sigma_{\mathbb{M}}$.

Definition 3.2 (δ -grid of lines). *Let $K \subset \mathbb{R}^n$ be a compact set and $\delta > 0$. The δ -grid of lines associated to K , denoted as $L_\delta(K)$, is a family of diagonal lines evenly sampled in K :*

$$L_\delta(K) := \{l_{\delta \cdot u} : u \in \mathbb{Z}^n \text{ and } l_{\delta \cdot u} \cap K \neq \emptyset\},$$

where $l_{\delta \cdot u} := \delta \cdot u + e_\Delta$ is the diagonal line with direction vector $e_\Delta = [1, \dots, 1]^T \in \mathbb{R}^n$ passing through $\delta \cdot u$.

Candidates decompositions. Our candidate decompositions are, roughly speaking, modules with the same fibered barcodes than \mathbb{M} on a δ -grid of lines. When \mathbb{M} is interval decomposable, we also ask the exact matchings induced by the candidate decompositions to commute with the one induced by \mathbb{M} (we discuss such matchings in Section 4.4).

Definition 3.3 (Candidate). *Let \mathbb{M} be a multi-parameter persistence module. Let K be a hyperrectangle in \mathbb{R}^n containing the multigraded Betti numbers of \mathbb{M} ², and $L := L_\delta(K^\delta)$ be the δ -grid of lines of the offset $K^\delta = \{x \in \mathbb{R}^n : d_\infty(x, K) \leq \delta\}$, where d_∞ stands for the $\|\cdot\|_\infty$ distance. A multi-parameter persistence module $\tilde{\mathbb{M}}_\delta$ is called a δ -candidate decomposition of \mathbb{M} if*

- (i) $\tilde{\mathbb{M}}_\delta$ is interval decomposable: $\tilde{\mathbb{M}}_\delta = \bigoplus_{i \in \tilde{\mathcal{I}}} \tilde{I}_i$,
- (ii) $\mathcal{B}(\mathbb{M}|_l) = \mathcal{B}(\tilde{\mathbb{M}}_\delta|_l)$ for any $l \in L$, i.e., their L -fibered barcodes are the same, and
- (iii) if $\mathbb{M} = \bigoplus_{i \in \mathcal{I}} I_i$ is interval decomposable, then there exists a bijection $\nu: \mathcal{I}_L \rightarrow \tilde{\mathcal{I}}$, where $\mathcal{I}_L = \{i \in \mathcal{I} : I_i \cap L \neq \emptyset\}$, such that $\text{supp}(I_i|_l) = \text{supp}(\tilde{I}_{\nu(i)}|_l)$, for any $i \in \mathcal{I}_L$ and $l \in L$. In particular, for any two lines $l, l' \in L$, the following diagram commutes:

$$\begin{array}{ccc} \mathcal{B}(\mathbb{M}|_l) & \xrightarrow{\sigma_{\mathbb{M}}} & \mathcal{B}(\mathbb{M}|_{l'}) \\ \downarrow \nu_l & & \downarrow \nu_{l'} \\ \mathcal{B}(\tilde{\mathbb{M}}_\delta|_l) & \xrightarrow{\sigma_{\tilde{\mathbb{M}}_\delta}} & \mathcal{B}(\tilde{\mathbb{M}}_\delta|_{l'}) \end{array}$$

where $\nu_l: I_i|_l \in \mathcal{B}(\mathbb{M}|_l) \mapsto \tilde{I}_{\nu(i)}|_l \in \mathcal{B}(\tilde{\mathbb{M}}_\delta|_l)$ (and similarly for l'). In other words, \mathbb{M} and $\tilde{\mathbb{M}}_\delta$ have the same matched barcodes along the lines of L , up to interval reordering.

We now claim that multi-parameter persistence modules that are δ -candidate decompositions of a given interval decomposable multi-parameter persistence module \mathbb{M} are δ close to \mathbb{M} in K , as stated in the following approximation result, which we prove in the next section.

Proposition 3.4 (Approximation result). *Let \mathbb{M} be an interval decomposable multi-parameter persistence module. Then, any δ -candidate decomposition $\tilde{\mathbb{M}}_\delta$ of \mathbb{M} satisfies*

$$d_1(\tilde{\mathbb{M}}_\delta \cap K, \mathbb{M} \cap K) \leq d_B(\tilde{\mathbb{M}}_\delta \cap K, \mathbb{M} \cap K) \leq \delta,$$

where $\mathbb{M} \cap K$ stands for the module that is isomorphic to \mathbb{M} on K and the null module outside of K .

Note that it is possible to generalize Proposition 3.4 to modules that are not restricted to K by constraining the parts of the candidate decompositions that are outside of K with Kan extensions, but we stick to our formulation for the sake of simplicity.

3.2 Proof of Proposition 3.4

In this section, we prove Proposition 3.4. This section is quite technical and can thus be skipped by readers who are most interested in the general exposition. We first provide several additional definitions in Section 3.2.1, that are a bit technical yet convenient for writing down the subsequent proofs. Then, we prove a few technical results and lemmas in Section 3.2.2, and we finally prove Proposition 3.4 in Section 3.2.3.

Notations. We first introduce a few notations: we let (e_1, \dots, e_n) be the canonical basis of \mathbb{R}^n , and, given a set $A \subseteq \mathbb{R}^n$, we let $\text{conv}(A)$ denote the convex hull of A . Moreover, given a hyperplane $H \subseteq \mathbb{R}^n$ and its two associated vectors $a_H, b_H \in \mathbb{R}^n$ which satisfy $H = b_H + \{x \in \mathbb{R}^n : \langle x, a_H \rangle = 0\}$, we call a_H the *codirection* of H . When a_H is a vector in the canonical basis of \mathbb{R}^n , i.e., there exists $i \in \llbracket 1, n \rrbracket$ such that $a_H = e_i$, we slightly abuse notation and also call i the codirection of H .

²See [BL22, Section 4.2] for the definition of multigraded Betti numbers. Note that understanding multigraded Betti numbers is not required to follow this work. Moreover, in practice, when \mathbb{M} is computed from the persistent homology of a multi-parameter filtration on a simplicial complex S induced by a continuous function f , it suffices to find a hyperrectangle K which contains all the multi-parameter filtration values, i.e., such that $\{f(\sigma) : \sigma \in S\} \subseteq K$.

3.2.1 Boundaries, facets and diagonal lines

In this section, we define the upper- and lower-boundaries of interval modules, as well as their so-called *facets*, which are convenient characterizations of the interval supports.

Definition 3.5 (Upper- and lower-boundaries). *Given an interval I , its upper-boundary $U[I]$ and lower-boundary $L[I]$ are defined as:*

$$L[I] := \{x \in \bar{I} : \forall y \in \mathbb{R}^n, y <_n x \Rightarrow y \notin I\}, \quad U[I] := \{x \in \bar{I} : \forall y \in \mathbb{R}^n, y >_n x \Rightarrow y \notin I\}$$

Moreover, the boundary of $\text{supp}(I)$ can be decomposed with $\partial\text{supp}(I) = L[I] \cup U[I]$. See Figure 2 for an illustration.

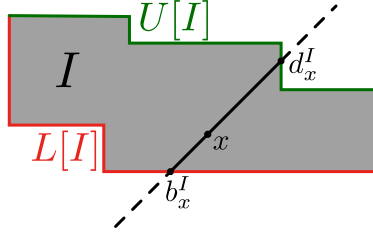


Figure 2: Lower- and upper-boundaries of a 2-interval (Definition 3.5); and birthpoints and deathpoints b_x^I and d_x^I (Definition 2.10) of a point $x \in \mathbb{R}^2$.

When interval modules are discretely presented (see Definition 2.7), their lower- and upper-boundaries are made of flat parts, which are the faces of the corresponding rectangles forming the interval. Hence, we call *facets* the subsets of the lower- and upper-boundaries that are included in some hyperplanes of \mathbb{R}^n .

Definition 3.6 (Facet). *A lower (resp. upper) facet of an interval I is an $(n-1)$ -submanifold of $\partial\text{supp}(I)$ written as $\{x \in \mathbb{R}^n : x_i = c\} \cap L[I]$ (resp. $\{x \in \mathbb{R}^n : x_i = c\} \cap U[I]$) for some $c \in \mathbb{R}$ and some dimension $i \in \llbracket 1, n \rrbracket$ that is called the facet codirection. In particular, the upper- and lower-boundaries of a discretely presented interval module is a locally finite union of facets.*

We end this section by defining some properties of diagonal lines.

Definition 3.7 (δ -regularly distributed lines filling a compact set). *Let L be a set of diagonal lines in \mathbb{R}^n and $K \subseteq \mathbb{R}^n$ be a compact set. Then, we say that :*

1. two diagonal lines $l, l' \in L$ are δ -consecutive (or consecutive when δ is clear) if there exists $\vec{u} \in \{0, 1\}^n \setminus \{0, 1\}$ such that $l' = l \pm \delta \cdot \vec{u}$.
2. two diagonal lines $l, l' \in L$ are δ -comparable if there exists a positive or negative vector $\vec{u} \in \mathbb{R}^n$ (i.e. a vector whose coordinates are all positive or all negative) with $\|\vec{u}\|_\infty \leq \delta$ such that $l' = l + \vec{u}$. If \vec{u} is positive (resp. negative), we write $l' \geq l$ (resp. $l' \leq l$).
3. L is δ -regularly distributed if, for any pair of lines $(l, l') \in L$, there exists a sequence of δ -consecutive lines $\{l_1, \dots, l_k\}$ in L such that $l = l_1$ and $l' = l_k$.
4. for a given line l in a δ -regularly distributed family of lines L , we call $L_l := L \cap \{l + \delta \cdot \vec{u} : \vec{u} \in \{0, 1\}^{n-1} \times \{0\}\}$ the L -surrounding set of l . In particular, one has $|L_l| \leq 2^{n-1}$.
5. L δ -fills K (or fills K when δ is clear) if any point of K is at distance at most $\delta/2$ from some line in L . More formally, K is included in the offset $L^{\delta/2}$.

Remark 3.8. *One can check that the δ -grid of lines of a hyperrectangle K (used in Definition 3.3) is δ -regularly distributed and δ -fills K .*

3.2.2 Additional lemmas

In this section, we prove a few preliminary results about endpoints of interval modules, that will turn out useful for proving Proposition 3.4. The first simple, yet fundamental lemma that we will use repeatedly states that endpoints of interval modules cannot be comparable.

Lemma 3.9. *Let l_1, l_2 be two diagonal lines and I be an interval module such that the barcodes $\mathcal{B}(I|_{l_1})$ and $\mathcal{B}(I|_{l_2})$ are not empty. Let $\mathcal{B}(I|_{l_1}) = [b_1, d_1]$ and $\mathcal{B}(I|_{l_2}) = [b_2, d_2]$. Then b_1 and b_2 are not comparable, i.e., $b_1 \not\leq_n b_2$ and $b_1 \not\geq_n b_2$. The same is true for d_1 and d_2 . In other words, the rectangles R_{b_1, b_2} , R_{b_2, b_1} , R_{d_1, d_2} and R_{d_2, d_1} are flat (i.e., one side has length 0).*

Proof. This lemma is a simple consequence of the persistence module definition: if b_1 and b_2 were comparable (as in Figure 3), then the rectangle R_{b_1, b_2} would not be trivial, and b_2 would not be a birthpoint since it would be possible to find a smaller birthpoint $\tilde{b}_2 \leq_n b_2$ w.r.t. the partial order of \mathbb{R}^n along the diagonal line passing through b_2 . A similar argument holds for d_1 and d_2 . See Figure 3.

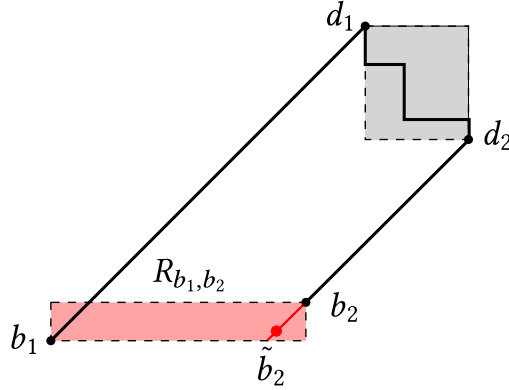


Figure 3: Two bars $[b_1, d_1]$ and $[b_2, d_2]$ of an interval module.

□

Stability of close barcodes. We now show that endpoints of bars in barcodes from lines that are close should also be close. In other words, bars of the fibered barcode that are associated to lines that are close to each other must have similar length, as stated in the lemma below (see also [Lan18, Lemma 2]).

Lemma 3.10. *Let I be an interval module, let $l_1, l_2 \subseteq \mathbb{R}^n$ be two diagonal lines and let $\vec{u} \in \mathbb{R}^n$ be a positive or negative vector (i.e., the coordinates of \vec{u} are either all positive or all negative) such that $l_2 = l_1 + \vec{u}$. Then, the following properties hold:*

- (i) *If the barcode $\mathcal{B}(I|_{l_1}) = \{[b_{i_1}^I, d_{i_1}^I]\}$ is not empty and satisfies $\|d_{i_1}^I - b_{i_1}^I\|_\infty > \|\vec{u}\|_\infty$, then the barcode $\mathcal{B}(I|_{l_2})$ is not empty as well, and*
- (ii) *If the barcodes $\mathcal{B}(I|_{l_1})$ and $\mathcal{B}(I|_{l_2})$ are not empty, then one has*

$$\|d_{i_1}^I - d_{i_2}^I\|_\infty \leq \|\vec{u}\|_\infty \quad \text{and} \quad \|b_{i_1}^I - b_{i_2}^I\|_\infty \leq \|\vec{u}\|_\infty,$$

where we used the conventions $(+\infty) - (+\infty) = (-\infty) - (-\infty) = 0$.

Proof. Item (i). Since $|(d_{i_1}^I)_i - (b_{i_1}^I)_i| = \|d_{i_1}^I - b_{i_1}^I\|_\infty > \|\vec{u}\|_\infty$ for any index $i \in \llbracket 1, n \rrbracket$, it follows that $b_{i_1}^I \leq_n b_{i_1}^I + \vec{u} \leq_n d_{i_1}^I$. Thus $b_{i_1}^I + \vec{u}$ must belong to $\text{supp}(I)$ since I is an interval. Hence, since $b_{i_1}^I + \vec{u} \in l_2$, one has $\mathcal{B}(I|_{l_2}) = \text{supp}(I) \cap l_2 \neq \emptyset$.

Item (ii). If one of the endpoints is infinite, the result holds trivially as the other endpoint has to be infinite too, so we now assume that the endpoints of the bars are all finite. Without loss of generality, assume that $l_2 = l_1 + \vec{u}$ where \vec{u} is positive. Now, since both $d_{l_2}^I$ and $d_{l_1}^I + \vec{u}$ belong to l_2 , they are comparable, so one has either $d_{l_2}^I >_n d_{l_1}^I + \vec{u}$ or $d_{l_2}^I \leq_n d_{l_1}^I + \vec{u}$. However, the first possibility would lead to $d_{l_2}^I >_n d_{l_1}^I + \vec{u} >_n d_{l_1}^I$, hence $d_{l_1}^I$ and $d_{l_2}^I$ would be (strictly) comparable in \mathbb{R}^n , which contradicts Lemma 3.9. Thus, one must have $d_{l_2}^I \leq_n d_{l_1}^I + \vec{u}$. Furthermore, and using the exact same arguments, $d_{l_2}^I - \vec{u} + \|\vec{u}\|_\infty \cdot \mathbf{1}$ is on l_1 , and one must have $d_{l_2}^I - \vec{u} + \|\vec{u}\|_\infty \cdot \mathbf{1} \geq_n d_{l_1}^I$. Finally, by combining the two previous inequalities, one has

$$d_{l_1}^I - \|\vec{u}\|_\infty \cdot \mathbf{1} \leq_n d_{l_1}^I + \vec{u} - \|\vec{u}\|_\infty \cdot \mathbf{1} \leq_n d_{l_2}^I \leq_n d_{l_1}^I + \vec{u} \leq_n d_{l_1}^I + \|\vec{u}\|_\infty \cdot \mathbf{1},$$

which leads to the result for deathpoints. The proof extends straightforwardly to birthpoints. \square

Endpoint location. The next definition and result show that endpoints of an interval module must be located in the vicinity of the other endpoints of the module that are close to it—more precisely, in their *rectangle hull*. This will be useful in the proof of Proposition 3.4; in particular, we will use this result to characterize the positions of endpoints of any given diagonal line l solely from the endpoints of the lines of the grid L that are close to l .

Definition 3.11. Let $S \subseteq \mathbb{R}^n$. The rectangle hull of S , denoted by $\text{recthull}[S]$, is defined as the smallest rectangle containing S

$$\text{recthull}[S] := \left\{ x \in \mathbb{R}^n : \forall i \in \llbracket 1, n \rrbracket, \min_{s \in S} s_i \leq x_i \leq \max_{s \in S} s_i \right\} = R_{\wedge S, \vee S},$$

where $(\wedge S)_i := \min_{s \in S} s_i$ and $(\vee S)_i := \max_{s \in S} s_i$.

Lemma 3.12 (Endpoints bound). Let I be an interval module. Let K be a hyperrectangle and $L = L_\delta(K^\delta)$ be a δ -grid of lines. Let $x \in K$, l_x be the diagonal line passing through x , and let $L_{x,\delta} := \{l \in L : d_\infty(x, l) \leq \delta \text{ and } l_x, l \text{ are } \delta\text{-comparable}\}$, which is non-empty since L δ -fills K . Assume that $l_x \cap \text{supp}(I) \neq \emptyset$, and $d_x^I \in U[I]$ be the associated deathpoint, and assume that for any line l in $L_{x,\delta}$, one has $\text{supp}(I) \cap l \neq \emptyset$, and let $D_{x,\delta}^I$ be the set of the associated deathpoints: $D_{x,\delta}^I = \{d_l^I : l \in L_{x,\delta}\}$. Then, d_x^I belongs to the rectangle hull of a subset $\tilde{D}_{x,\delta}^I$ of $D_{x,\delta}^I$: one has $d_x^I \in \text{recthull}[\tilde{D}_{x,\delta}^I]$ with $\tilde{D}_{x,\delta}^I \subseteq D_{x,\delta}^I$.

Similarly, if $b_x^I \in L[I]$ is a birthpoint, then $b_x^I \in \text{recthull}[\tilde{B}_{x,\delta}^I]$, where $\tilde{B}_{x,\delta}^I$ is a subset of $B_{x,\delta}^I = \{b_l^I : l \in L_{x,\delta}\}$, i.e., the set of birthpoints associated to $L_{x,\delta}$.

In other words, the endpoints of an interval module always belong to the rectangle hull of the endpoints associated to neighbouring lines. See Figure 4 for an illustration.

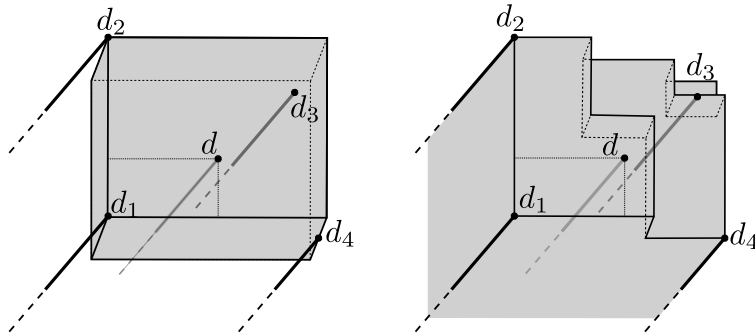


Figure 4: Example of deathpoint bound in \mathbb{R}^3 , with $d \in U[I]$, and $D_{x,\delta}^I = \{d_1, d_2, d_3, d_4\}$. **(Left)** Rectangle hull of the deathpoints $D_{x,\delta}^I$. **(Right)** Upper-boundary $U[I]$.

Proof. We first prove the result for deathpoints. Note that the result is trivially satisfied if d_x^I and the deathpoints in $D_{x,\delta}^I$ are infinite, so we assume that they are finite in the following. To alleviate notations, we let $d := d_x^I$. Let $j \in \llbracket 1, n \rrbracket$ be an arbitrary dimension. In order to prove the result, we will show that there exist two deathpoints \underline{d} and \bar{d} associated to consecutive lines of $L_{x,\delta}$ such that $\underline{d}_j \leq d_j \leq \bar{d}_j$.

Construction of \underline{d}, \bar{d} . Let H_j be the hyperplane $H_j = d + e_j^\perp$. Since L δ -fills K , there exists a diagonal line $l \in L$ such that $d_\infty(x, l) \leq \delta/2$. Moreover, since l and l_x (the line passing through x and d) are both diagonal, one has $d_\infty(d, l) = d_\infty(x, l) \leq \delta/2$. Let $\pi_l(d) \in l$ be the projection of d onto l that achieves $d_\infty(d, l)$, and let $d^j := l \cap H_j$. See Figure 5 for an illustration of these objects.

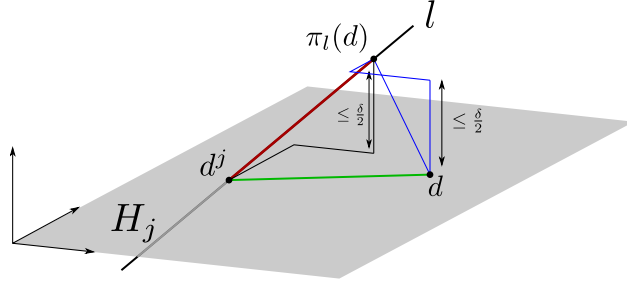


Figure 5: Illustration of H_j, d, l, d^j .

Since d^j and d belong to H_j , they have the same j -th coordinate: $d_j^j = d_j$. Moreover, both d^j and $\pi_l(d)$ belong to the diagonal line l , hence they are comparable, and $\|d^j - \pi_l(d)\|_\infty = |(d^j - \pi_l(d))_i|$ for any $i \in \llbracket 1, n \rrbracket$. Then, one has $\|d^j - d\|_\infty \leq \|d^j - \pi_l(d)\|_\infty + \|\pi_l(d) - d\|_\infty = |(d^j - \pi_l(d))_j| + \|\pi_l(d) - d\|_\infty = |(d - \pi_l(d))_j| + \|\pi_l(d) - d\|_\infty \leq 2\|\pi_l(d) - d\|_\infty \leq \delta$.

Let $d^+ = d^j + \delta \sum_{j \in \mathcal{J}''} e_j$ and $d^- = d^j - \delta \sum_{j \in \mathcal{J}' } e_j$, where

$$\mathcal{J}' = \left\{ i \in \llbracket 1, n \rrbracket \setminus \{j\} : d_i < d_i^j \right\} \quad \text{and} \quad \mathcal{J}'' = \left\{ i \in \llbracket 1, n \rrbracket \setminus \{j\} : d_i > d_i^j \right\}.$$

By construction, one has $d^- \leq d \leq d^+ \in H_j$ and

$$\|d^+ - d\|_\infty, \|d^- - d\|_\infty \leq \delta. \quad (4)$$

Since l and the diagonal lines \underline{l} and \bar{l} passing through d^- and d^+ respectively are δ -consecutive, and since $x \in K$, the projections of x onto \underline{l} and \bar{l} are in K^δ , and thus \underline{l}, \bar{l} must belong to L , and thus to $L_{x,\delta}$, as by construction l_x is δ -comparable with the diagonal lines \underline{l} and \bar{l} . Let $\bar{d} := d_{\underline{l}}^I \in \underline{l}$ and $\underline{d} := d_{\bar{l}}^I \in \bar{l}$ be their deathpoints (which exist by assumption).

Proof of inequalities. We now show that $\bar{d}_j \geq_n d_j \geq_n \underline{d}_j$. We start with the second inequality. Since d^+ and \underline{d} are one the same diagonal line, they are comparable. Furthermore, if one had $d^+ <_n \underline{d}$ by contradiction, then the induced rectangle $R_{d,\underline{d}}$ would not be flat since $d \leq_n d^+ <_n \underline{d}$, which would contradict Lemma 3.9. As a consequence, $d^+ \geq_n \underline{d}$. Taking the j -th coordinate yields $d_j = d_j^+ \geq \underline{d}_j$. The first inequality holds using the same arguments.

This proof applies straightforwardly to birthpoints by symmetry. \square

Using Lemma 3.10, one can generalize Lemma 3.12 above to the case where some lines in $L_{x,\delta}$ have an empty intersection with $\text{supp}(I)$, and then define a common location for all endpoints that belong to the convex hull of the same L -surrounding set, as we do in the following proposition.

Proposition 3.13. *Let I be an interval module. Let K be a hyperrectangle and $L = L_\delta(K^\delta)$ be a δ -grid of lines. Let $l \in L$ such that $|L_l| = 2^{n-1}$ and assume that $\text{conv}(L_l) \cap L[I]$ (resp. $\text{conv}(L_l) \cap U[I]$) is not empty.*

Then, there exists a set B_l (resp. D_l) such that for any $x \in \text{conv}(L_l) \cap L[I]$ (resp. $\text{conv}(L_l) \cap U[I]$), one has either $\|b_x^I - d_x^I\|_\infty \leq \delta$, or $x \in B_l$ (resp. D_l), where B_l (resp. D_l) is a rectangular set in \mathbb{R}^n that can be constructed from the birthpoints $(b_{l'}^I)_{l' \in L_l}$ (resp. deathpoints $(d_{l'}^I)_{l' \in L_l}$). Moreover, one has that

$$\text{diam}(B_l) = \sup_{x, x' \in B_l} \|x - x'\|_\infty \leq \delta, \quad (5)$$

and similarly for D_l .

Proof. We first construct B_l and D_l , and then we will show items (1) and (2).

Definition of B_l, D_l . Let first assume that x is in the interior of $\text{conv}(L_l)$, that we denote with $\text{conv}(L_l)^\circ$. Note that if there is a line l_0 that is δ -comparable to l_x , and such that $\mathcal{B}(I|_{l_0}) = \emptyset$, then by Lemma 3.10 (i), one immediately has $\|b_x^I - d_x^I\|_\infty \leq \delta$. Hence, we now assume that the barcodes along any line that is δ -comparable to l_x is not empty, which means that the hypotheses of Lemma 3.12 are satisfied for x . Now, remark that since L is a grid, if one is able to find a line l' in L whose intersections with hyperplanes associated to the canonical axes of \mathbb{R}^n are δ -close to x , then, since x is in the interior of an L -surrounding set L_l , l' must belong to that surrounding set L_l as well. More formally, one has that, for any line $l' \in L$,

$$d_\infty(x, l' \cap H_i) \leq \delta \implies l' \in L_l, \quad \text{where } H_i = \{y \in \mathbb{R}^n : y_i = x_i\}.$$

This ensures (from Equation 4) that the lines of L associated to $\tilde{B}_{x, \delta}^I$ and $\tilde{D}_{x, \delta}^I$ are all included in L_l for any $x \in \text{conv}(L_l)^\circ$, and thus that we can safely define

$$D_l := \overline{\bigcup_{x \in \text{conv}(L_l)^\circ} \text{recthull}[\tilde{D}_{x, \delta}^I]} \quad \text{and} \quad B_l := \overline{\bigcup_{x \in \text{conv}(L_l)^\circ} \text{recthull}[\tilde{B}_{x, \delta}^I]}.$$

Note that B_l and D_l depend only on the endpoints of the lines in L_l and that $d_x^I \in D_l$ and $b_x^I \in B_l$ for any $x \in \text{conv}(L_l)^\circ$ by Lemma 3.12. Furthermore, if x is in the closure of $\text{conv}(L_l)$, the previous statements still hold since D_l and B_l are closed sets. We now show that B_l and D_l satisfy Equation (5).

Proof of Equation (5). By applying Lemma 3.12 and its proof for arbitrary dimension j to all $x \in \text{conv}(L_l) \cap U[I]$, there exist deathpoints \bar{d}^j and \underline{d}_j that satisfy $(\bar{d}^j)_j = \sup_{d \in D_l} d_j$ and $(\underline{d}_j)_j = \inf_{d \in D_l} d_j$ and $(\underline{d}_j)_j \leq x_j \leq (\bar{d}^j)_j$ for all $x \in \text{conv}(L_l) \cap U[I]$. Moreover, these points are located on lines in L_l that are δ -consecutive by definition. Thus, applying Lemma 3.10 (ii) repeatedly on these pairs of lines for all dimensions, we end up with D_l having a diagonal smaller than δ . The same goes for birthpoints. □

3.2.3 Proof of Proposition 3.4

Proof. Let $\mathbb{M} = \bigoplus_{i \in \mathcal{I}} I_i$ and $\tilde{\mathbb{M}}_\delta = \bigoplus_{i \in \tilde{\mathcal{I}}} \tilde{I}_i$ be the interval decompositions of \mathbb{M} and $\tilde{\mathbb{M}}_\delta$, with induced exact matchings $\sigma_{\mathbb{M}}$ and $\sigma_{\tilde{\mathbb{M}}_\delta}$ respectively. In order to upper bound the bottleneck distance $d_B(\mathbb{M}, \tilde{\mathbb{M}}_\delta)$, one can upper bound the interleaving distance $d_I(I_i, \tilde{I}_{\nu(i)})$ for any index $i \in \mathcal{I}$. Let I and \tilde{I} be two such intervals (we drop the index i to alleviate notations). Since I and \tilde{I} are interval modules, and thus indicator modules, the morphisms $\varphi_{I \rightarrow \tilde{I}}^{(\delta)} : I \rightarrow \tilde{I}(\delta)$ and $\varphi_{\tilde{I} \rightarrow I}^{(\delta)} : \tilde{I} \rightarrow I(\delta)$ are well-defined. We thus need to show that these morphisms commute, i.e., that they induce a δ -interleaving. Hence, we first show that

$$\left(\varphi_{\tilde{I} \rightarrow I}^{(\delta)}\right)_{x+\delta} \circ \left(\varphi_{I \rightarrow \tilde{I}}^{(\delta)}\right)_x = \left(\varphi_I^{(2\delta)}\right)_x, \quad (6)$$

for any $x \in K$.

If $x \in l$ for some line $l \in L$, Equation (6) is satisfied from $\text{supp}(I) \cap l = \text{supp}(\tilde{I}) \cap l$, which itself comes from the fact that \mathbb{M}_δ has the same L -fibered barcode than \mathbb{M} . Hence, we assume in the following that $x \notin \cup_{l \in L} l$. Furthermore, if $x \notin \text{supp}(I)$ or $x + 2\delta \notin \text{supp}(I)$, then Equation (6) is trivially satisfied. Hence, we also assume $x, x + 2\delta \in \text{supp}(I)$. This means that b_x^I and d_x^I are well-defined, and that $\left(\varphi_I^{(2\delta)}\right)_x \cong \text{id}_{k \rightarrow k}$. Thus we only have to show that $\tilde{I}_{x+\delta} \cong k$, i.e., $x + \delta \in \text{supp}(\tilde{I})$.

As $L = L_\delta(K^\delta)$ is the δ -grid of K^δ and $x \in K$, let $l \in L$ be a line such that $x \in \text{conv}(L_l)$ and let $l_x \subseteq \text{conv}(L_l)$ be the diagonal line passing through x . Now, as $R_{x, x+\delta} \subseteq \text{supp}(I)$, Lemma 3.10 (i) ensures that $\mathcal{B}(I|_{l_x}) \neq \emptyset$ for any line $l \in L$ that is δ -comparable to l_x ; and the same holds for \tilde{I} since $\mathcal{FB}(I)_L = \mathcal{FB}(\tilde{I})_L$. Using Proposition 3.13 on both I and \tilde{I} , there exist two sets B_l and D_l such that $d_x^I, d_x^{\tilde{I}} \in D_l$ and $b_x^I, b_x^{\tilde{I}} \in B_l$, with the segments $l_x \cap B_l$ and $l_x \cap D_l$ having length at most δ . Since one also has

$$b_x^I \leq x \leq x + 2\delta \leq d_x^I,$$

and $\left\|d_x^I - d_x^{\tilde{I}}\right\|_\infty, \left\|b_x^I - b_x^{\tilde{I}}\right\|_\infty \leq \delta$, one finally has $b_x^{\tilde{I}} \leq x + \delta \leq d_x^{\tilde{I}}$, which concludes that $x + \delta \in \text{supp}(\tilde{I})$. \square

4 Computing stable candidate decompositions with MMA

In this section, we first introduce the general problem of computing candidate decompositions (see Definition 3.3) in Section 4.1, and we introduce our algorithm MMA for computing instances of candidate decompositions on any multi-parameter persistence module in arbitrary dimension, i.e., with arbitrary number of filtrations, in Section 4.2. In particular, one does not have to assume that the underlying module is decomposable in order to run MMA. When the underlying module is interval decomposable, we show that our algorithm MMA can actually recover it exactly in Section 4.3. Finally, even when the underlying module is not necessarily interval decomposable, we also show that the candidate decompositions computed by MMA are still stable in Section 4.4.

4.1 Motivation

The goal of this section is to frame the general question of practically computing candidate decompositions of a multi-parameter persistence module from its fibered barcode. There are many ways of doing so, but the most natural ones are not necessarily the easiest computable ones. For the sake of simplicity, let us leave the problem of finding proper matching functions aside for now (which we will discuss in more details in Section 5), and assume that the underlying module is a single interval module $\mathbb{M} = I$. Since interval modules are characterized by their supports, the goal is to recover $\text{supp}(I)$. Moreover, if I is discretely presented, only the facets and critical points of $\text{supp}(I)$ need to be captured or approximated. There are many different ways, for a given interval module I , to define candidate critical points, that we call *corners*, using the endpoints of its fibered barcode, e.g., by using the minimum and maximum of consecutive endpoint coordinates. Hence, it is natural to define candidate decompositions (or candidate approximations in this case, since there is just one summand) \tilde{I} with model selection, i.e., by minimizing some penalty cost $\text{pen}: S \rightarrow \mathbb{R}_+$, where S is the set of discretely presented interval modules having the same fibered barcode as I , or a subset thereof. See Figure 6 for examples of sets S and corresponding candidate approximations. This penalty would forbid, e.g., overly complicated approximations that have a lot of corners. For instance, minimizing the penalty

$$\text{pen} : \tilde{I} \mapsto \#\text{corners of } \text{supp}(\tilde{I}). \quad (7)$$

would provide a sparse approximation of I . Actually, when one assumes that the underlying interval module I is discretely presented with facets that are large enough with respect to the family of lines L of the fibered barcode, the target I minimizes penalty (7). Indeed, as all the facets of I are detected by some endpoints of

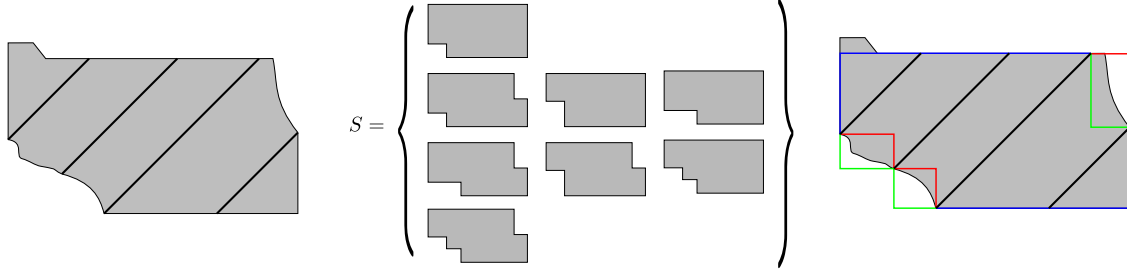


Figure 6: Example of candidates for a 2-interval module I with support in \mathbb{R}^2 . **(Left)** Given the L -fibered barcode of I , where L is the family of the four black lines, we want to approximate I with an element of S , i.e., an interval module with the same fibered barcode. **(Middle)** When one further constrains the set S by asking to have at most one corner between two consecutive endpoints of the fibered barcode, the whole set S can be computed explicitly. **(Right)** The set S can also be described as the set of intervals which have to go through the blue path, and which can arbitrarily choose between the red or green path at three different locations. Hence, the cardinality of S is 2^3 .

the fibered barcode by assumption, any candidate approximation \tilde{I} of I has at least the same number of facets than I , i.e., $\text{pen}(I) \leq \text{pen}(\tilde{I})$ for any candidate approximation \tilde{I} .

For interval modules, S is generally a set of cardinal c^d , where c is the number of candidate corners between birthpoints or deathpoints, and d is the number of corners. For instance, in Figure 6, one has $n = 2$, $c = 2$ and $d = 3$. Unfortunately, c is of the order of 2^{n-1} , and thus grows exponentially with the dimension n , and d is difficult to control in practice, since it heavily depends on the number of lines in the fibered barcode and the regularity of the underlying interval module I . Minimizing a penalty over S is thus practical only for low dimension n and small number of lines in the fibered barcode. Hence, our algorithm **MMA** presented in Section 4.2 does not use penalty minimization, but is rather defined with natural and simple corner choices.

Remark 4.1. Note also that there are cases when the corner choices are canonical. For instance, any 2-multipersistence module M with transition maps φ that are weakly exact, i.e., that satisfy, for any $x \leq y$

$$\text{im}(\varphi_x^y) = \text{im}(\varphi_{(y_1, x_2)}^y) \cap \text{im}(\varphi_{(x_1, y_2)}^y) \quad \text{and} \quad \ker(\varphi_x^y) = \ker(\varphi_{(y_1, x_2)}^y) + \ker(\varphi_{(x_1, y_2)}^y),$$

is rectangle decomposable [BLO22]. Hence, a canonical approximation of a summand I of \mathbb{M} is given by the interval module whose support is the rectangle with corners $(\min_l(b_l^I)_1, \min_l(b_l^I)_2)$ and $(\max_l(b_l^I)_1, \max_l(b_l^I)_2)$, where l goes through the family of lines L of the fibered barcode.

4.2 MMA algorithm for computing candidate decompositions

In this section, we introduce **MMA**: a fast algorithm for computing δ -candidate decompositions. The pseudo-code for **MMA** is provided in Algorithm 1. Roughly speaking, given a multi-parameter persistence module \mathbb{M} , an approximation parameter $\delta > 0$, a δ -grid of lines $L = L_\delta(K^\delta)$ where K contains the multigraded Betti numbers of \mathbb{M} , and a matching function σ that commutes with the exact matching function $\sigma_{\mathbb{M}}$ induced by \mathbb{M} (see Section 5 for a discussion about how to find such matching functions), Algorithm 1 works in three steps:

Step 1: compute the L -fibered barcode of \mathbb{M} ,

Step 2: match together bars that correspond to the same underlying summand using the matching function σ ,

Step 3: for each summand, use the endpoints of the corresponding bars to compute estimates of the critical points, using Algorithm 2.

Step 1 can be performed using any persistent homology software (such as, e.g., `Gudhi`, `Ripser`, `Phat`, etc), or with `Rivet` [LW15] when $n = 2$. Our code can be found at <https://github.com/DavidLapous/multipers>, and is based on the vineyard algorithm [CSEM06], which allows us to run Steps 1 and 2 jointly (see Section 5.2).

Algorithm 1: MMA: Multi-parameter persistence Module Approximation.

Input 1: A multi-parameter persistence module \mathbb{M} (whose multigraded Betti numbers are included in a hyperrectangle K),
Input 2: δ -grid of evenly spaced diagonal lines $L = L_\delta(K^\delta)$
Input 3: Matching function σ (commuting with $\sigma_{\mathbb{M}}$ if \mathbb{M} is interval decomposable)
Output: Candidate decomposition $\tilde{\mathbb{M}}_\delta$
Compute $\mathcal{FB}(\mathbb{M})_L = \mathcal{FB}(\mathcal{M})_L$, i.e., the L -fibered barcode of \mathbb{M} ;
 $S \leftarrow []$; # S is the set of interval summands of the output candidate decomposition, initialized as the empty set
for $l \in L$ **do**
 for $[b_l^{\mathbb{M}}, d_l^{\mathbb{M}}] \in \mathcal{B}(\mathbb{M}|_l)$ **do**
 # Check whether it is in the image of the input matching
 if $\exists B \in S$ and $[b, d] \in B$ s.t. $[b_l^{\mathbb{M}}, d_l^{\mathbb{M}}] = \sigma([b, d])$ **then**
 | $B.append([b_l^{\mathbb{M}}, d_l^{\mathbb{M}}])$; # If it is, attach the bar to the corresponding summand
 # Otherwise initialize a new summand with the bar
 else
 | Add $B := \{[b_l^{\mathbb{M}}, d_l^{\mathbb{M}}]\}$ to S ;
 # For each summand in S characterized by a set of bars, build an approximate interval summand
Return $\tilde{\mathbb{M}}_\delta := \bigoplus_{B \in S} \text{APPROXIMATEINTERVAL}(B)$;

We now describe the algorithm `APPROXIMATEINTERVAL`, which is used at the end of Algorithm 1. Its pseudo-code is given in Algorithm 2, and is defined in two steps:

1. first, we *label* birthpoints and deathpoints to identify facets with `LABELENDPOINTS` (Algorithm 3),
2. then, we use these labels to compute candidate critical points with `COMPUTECORNERS` (Algorithm 4).

Algorithm 2: `APPROXIMATEINTERVAL`

Input: Set of bars $B = \{[b_l, d_l]\}_{l \in L_B}$, where $L_B \subseteq L$
Output: Discretely presented interval module \tilde{I}
 $\text{LABS} \leftarrow \text{LABELENDPOINTS}(B)$;
 $C_B^L(I), C_D^L(I) \leftarrow \text{COMPUTECORNERS}(B, \text{LABS})$;
Return $\tilde{I}(B) := \text{Int} \left(\bigcup_{c \in C_B^L(I)} \bigcup_{c' \in C_D^L(I)} R_{c, c'} \right)$;

We first describe `LABELENDPOINTS`. The core idea of this algorithm, whose pseudo-code is given in Algorithm 3, is, for a given bar in I associated to a line $l \in L$, to look at the corresponding surrounding set L_l . If there exists a hyperplane H such that all endpoints in this surrounding set belong to H , we identify H as a facet, and we label the bar with the codirection of H .

Algorithm 3: `LABELENDPOINTS`

Input: Set of bars $B = \{[b_l, d_l]\}_{l \in L_B}$, where $L_B \subseteq L$
Output: List LABS of labels for each endpoint in B
 $\text{LABS}(b_l) \leftarrow []$ for all $l \in L_B$;
for $l \in L_B$ **do**
 if $\exists i \in [1, n]$ and $c_i \in \mathbb{R}$, such that $\forall l' \in L_l$, $(b_{l'})_i = c_i$ **then**
 | Add (i, c_i) to $\text{LABS}(b_{l'})$ for all $l' \in L_l$;
Return LABS ;

Note that endpoints can have zero or more than one label. For instance, an endpoint that belongs to the intersection of several facets might have multiple labels. However, if several labels are identified, they must be associated to different dimensions. See Figure 7 for examples of label assignments when the underlying interval module has rectangle support.

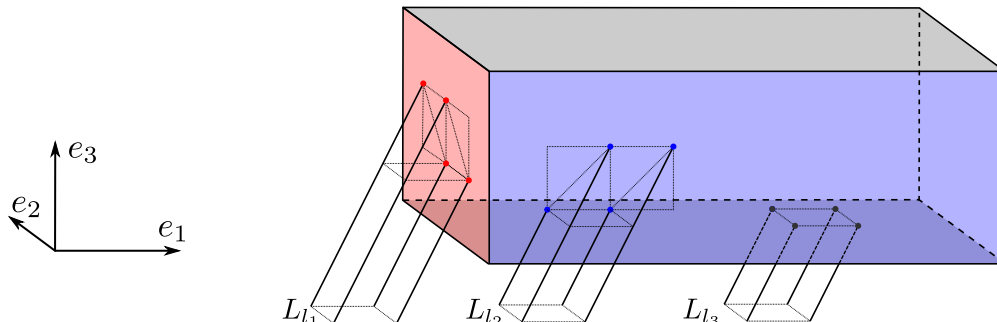


Figure 7: Example of birthpoint labelling for an interval module I with rectangle support with three surrounding sets of lines L_{l_1} , L_{l_2} , L_{l_3} associated to three lines l_1, l_2, l_3 . The labels of l_1, l_2, l_3 that are identified correspond to the red, blue and grey colored facets of I respectively.

Finally, we describe COMPUTECORNERS. The core idea of the algorithm, whose pseudo-code is given in Algorithm 4, is to use the labels identified by LABELENDPOINTS to compute *corners*, or critical point estimates, in the following way: if all birthpoints (resp. deathpoints) in a surrounding set have at least one associated facet, i.e., have a non-empty list of labels, then a candidate corner can be defined using the minimum (resp. maximum) of all birthpoints (resp. deathpoints) coordinates. We only present the pseudo-code for birthpoints since the code for deathpoints is symmetric and can be obtained by replacing minimum by maximum and $-\infty$ by $+\infty$.

Complexity. Computing the L -fibered barcode $\mathcal{FB}(\mathbb{M})_L$ on a simplicial complex, as well as assigning the corresponding bars to their associated summands in the decomposition of \mathbb{M} , can be done with the vineyard algorithm and matching [CSEM06] with complexity $O(N^3 + |L| \cdot N \cdot T)$, where N is the number of simplices in the simplicial complex, and T is the maximal number of transpositions required to update the single-parameter filtrations corresponding to the consecutive lines in L . In the worst case scenario, $T = N^2$. Note that T usually decreases to a fixed constant as $|L|$ increases, and that this computation can be easily parallelized in practice.

Now, adding the complexities of Algorithms 3 and 4, the final complexity of Algorithm 1 is

$$O(N^3 + |L| \cdot N \cdot T + |L| \cdot n \cdot 2^{n-1}). \quad (8)$$

Of importance, the dependence on n is much better than the (exact) decomposition algorithm proposed in [DX22] whose complexity is $O(N^{n(2\omega+1)})$, where $\omega < 2.373$ is the matrix multiplication exponent. It is also comparable to Rivet [LW15] (which works only when $n = 2$), whose complexity is $O(N^3\kappa + (N + \log\kappa)\kappa^2)$, where $\kappa = \kappa_x\kappa_y$ is the product of x and y coordinates used to evaluate the module (note that κ_x, κ_y are also user-dependent). The elder-rule staircase [CKMW20] works only for point cloud data when $n = 2$ and homology dimension 0, but has better complexity $O(m^2 \log(m))$, where m is the number of points. Finally, note that our complexity can be controlled by the number of lines, which is user-dependent. We illustrate this useful property in Section 6.

Remark 4.2. For the sake of simplicity and efficiency, the code that we provide at <https://github.com/DavidLapous/multipers> contains a simpler version of Algorithm 4, that does not compute and use labels, but rather gathers the birthpoints and deathpoints as corners directly. One can easily check that the correctness result (Proposition 4.3 and its proof below) carries over to that simpler algorithm, however the exactness result (Corollary 4.10 below) is only valid for corners computed with Algorithm 4.

Algorithm 4: COMPUTECORNERS

Input 1: Set of bars $B = \{[b_l, d_l]\}_{l \in L_B}$, where $L_B \subseteq L$

Input 2: List LABS of labels for each endpoint in B

Output: List of birth corners C_B

$C_B \leftarrow []$;

for $l \in L_B$ **do**

$B_{L_l} \leftarrow \{b_{l'} : l' \in L_l \cap L_B\}$; # Note that $B_{L_l} \subseteq B$ by construction

 # Check whether all birthpoints in the surrounding set belong to K

if $B_{L_l} \subseteq K$ **then**

 # Compute birth corner if all the birthpoints are labelled

if $\text{LABS}(b) \neq \emptyset, \forall b \in B_{L_l}$ **then**

$\{(j, c_j) : j \in \mathcal{J}\} \leftarrow \bigcup_{b \in B_{L_l}} \text{LABS}(b)$; # $\mathcal{J} \subseteq [1, n]$ is the set of codirections

 Define $C^l \in \mathbb{R}^n$ as

- $(C^l)_j = c_j$ if $j \in \mathcal{J}$
- $(C^l)_j = \min \{(b_{l'})_j : l' \in L_l \cap L_B\}$ otherwise

$C_B.\text{append}(C^l)$;

 # If the birthpoints are not all labeled, keep the birthpoints themselves as corners

else

for $l' \in L_l \cap L_B$ **do**

$C_B.\text{append}(b_{l'})$;

 # If some birthpoints are not in K , they must correspond to infinite facets

else

Assert $B_{L_l} \cap K^\delta \setminus K \neq \emptyset$;

Assert $\text{LABS}(b) \neq \emptyset$ for all $b \in B_{L_l}$;

$\{(j, c_j) : j \in \mathcal{J}\} \leftarrow \bigcup_{b \in B_{L_l}} \text{LABS}(b)$; # The cardinality of the set of codirections $\mathcal{J} \subsetneq [1, n]$ must be strictly less than n

 Define $C^l \in \mathbb{R}^n$ as

- $(C^l)_j = c_j$ if $j \in \mathcal{J}$
- $(C^l)_j = -\infty$ otherwise

$C_B.\text{append}(C^l)$;

Return C_B ;

Correctness of MMA. The following proposition ensures that MMA is correct.

Proposition 4.3. *Let \mathbb{M} be an interval decomposable multi-parameter persistence module. Let $\tilde{\mathbb{M}}_\delta^{\text{MMA}} = \text{MMA}(\mathbb{M}, L_\delta(K^\delta), \sigma)$, where σ commutes with $\sigma_{\mathbb{M}}$. Then $\tilde{\mathbb{M}}_\delta^{\text{MMA}}$ is a δ -candidate decomposition of \mathbb{M} .*

Proof. Let I be an interval summand of \mathbb{M} , and \tilde{I} be the associated interval summand of the candidate decomposition $\tilde{\mathbb{M}}_\delta^{\text{MMA}}$ (which is well-defined as σ is assumed to commute with $\sigma_{\mathbb{M}}$). Let $C_B^I(I)$ and $C_D^I(I)$ be the birth and death corners computed by Algorithm 4, i.e., one has

$$\tilde{I} = \text{Int} \left(\bigcup_{c \in C_B^I(I)} \bigcup_{c' \in C_D^I(I)} R_{c, c'} \right), \quad (9)$$

In order to show that $\tilde{\mathbb{M}}_\delta^{\text{MMA}}$ is a δ -candidate decomposition of \mathbb{M} , it suffices to show that the L -fibered barcodes of \tilde{I} and I are the same, i.e., $\mathcal{FB}(I)_L = \mathcal{FB}(\tilde{I})_L$. Equivalently, we need to show that $\text{supp}(I) \cap l = \text{supp}(\tilde{I}) \cap l$ for any line $l \in L$. We first show that they share the same birthpoints, i.e., that

$L[I] \cap L = L[\tilde{I}] \cap L$. Let $l \in L$. Note that b_l^I and $b_l^{\tilde{I}}$ are comparable since they belong to the same diagonal line l .

Strategy. In order to show $b_l^{\tilde{I}} = b_l^I$, we are going to show that 1. $b_l^I \leq_n b_l^{\tilde{I}}$ and 2. $b_l^{\tilde{I}} \leq_n b_l^I$.

1. In order to show $b_l^I \leq_n b_l^{\tilde{I}}$, we are going to show that $c \not\leq_n b_l^I$ for any corner $c \in C_B^L(I)$. Indeed, if one assumes $b_l^I >_n b_l^{\tilde{I}}$, and since there always exists a birth corner $c \in C_B^L(I)$ such that $c \leq_n b_l^{\tilde{I}}$ by construction of \tilde{I} , one has $c \leq_n b_l^{\tilde{I}} <_n b_l^I$.
2. In order to show $b_l^{\tilde{I}} \leq_n b_l^I$, we are going to show that there exists a corner $c \in C_B^L(I)$ such that $c \leq_n b_l^I$. Indeed, if there is such a birth corner, and if $b_l^{\tilde{I}} >_n b_l^I$ by contradiction, then $c \leq_n b_l^I <_n b_l^{\tilde{I}}$, and $R_{c, b_l^{\tilde{I}}}$ is not flat, contradicting Lemma 3.9.

Proof of (2). By construction of \tilde{I} with Algorithm 4, if b_l^I is labelled, then there exists a line l' and a corner $c' \in C_B^L(I)$ that is smaller than b_l^I so we can take $c := c'$. If b_l^I is not labelled, it belongs itself to $C_B^L(I)$, and we can take $c := b_l^I$.

Proof of (1). Let $c \in C_B^L(I)$ be a birth corner, and let L_{l_0} be the associated surrounding set of lines for some $l_0 \in L$. Let $[c]_l := \min [(c + (\mathbb{R}_+)^n) \cap l]$ be the smallest element in the intersection between the positive cone on c and l . Assume $[c]_l \geq_n b_l^I$ and $c <_n b_l^I$. Then $R_{c, [c]_l}$ is not flat, contradicting the fact that $[c]_l$ is the smallest element. Thus, we only have to show $[c]_l \geq_n b_l^I$. There are two cases.

- Either some birthpoints of L_{l_0} are not labelled by Algorithm 3, and c is equal to $b_{l'}^I$ for some $l' \in L_{l_0}$. Now, assume $[c]_l <_n b_l^I$ by contradiction. Then $b_{l'}^I = c \leq_n [c]_l <_n b_l^I$. Thus $b_{l'}^I <_n b_l^I$ and $R_{b_{l'}^I, b_l^I}$ is not flat, contradicting Lemma 3.9. Hence $[c]_l \geq_n b_l^I$.
- Or all the birthpoints of L_{l_0} are labelled by Algorithm 3. Again, we study two separate cases. See Figure 8 for an illustration.
 - Either $l \in L_{l_0}$. Then, $\exists i \in \llbracket 1, n \rrbracket$ such that $(b_l^I)_i = c_i$. This yields $(b_l^I)_i = c_i \leq ([c]_l)_i$, and thus $[c]_l \geq_n b_l^I$ since they both belong to the same diagonal line l .
 - Or the line l does not belong to L_{l_0} . Since $[c]_l$ is on the boundary of the positive cone based on c , there exists $i \in \llbracket 1, n \rrbracket$ such that $([c]_l)_i = c_i$. Assume again by contradiction that $b_l^I >_n [c]_l$, and write

$$[c]_l = c + \sum_{j \neq i} (\delta \alpha_j) e_j =: c + \vec{v} <_n b_l^I$$

with $\alpha_j \geq 0$ for $j \in \llbracket 1, n \rrbracket \setminus \{i\}$. Since $l \notin L_{l_0}$, there exists some j_0 such that $\alpha_{j_0} > 1$. Let $\vec{u} := ((\vec{v}_j \bmod \delta)_{j \in \llbracket 1, n \rrbracket}) = (([c]_l - c)_j \bmod \delta)_{j \in \llbracket 1, n \rrbracket} \in [0, \delta)^n \leq_n \vec{v}$. Let $l' := l_{c + \vec{u}}$ be the diagonal line passing through $c + \vec{u}$. Now, recall that the lines of L are drawn on a grid, so $l' \in L$ since $l' = l + \vec{u} - \vec{v}$. Moreover, one has by definition, $c \in \text{conv}(L_{l_0})$. Since the lines of L are on a grid, one has

$$\forall l_1, l_2 \in L, \|l_1 \cap H_n, \text{conv}(L_{l_2}) \cap H_n\|_\infty < \delta \implies l_1 \in L_{l_2},$$

where $H_n = \{x \in \mathbb{R}^n : x_n = c_n\}$. Now, note that $c + \vec{u}$ and $c + \vec{u} - \vec{u}_n \cdot \mathbf{1}$ both belong to l' , and that $c + \vec{u} - \vec{u}_n \cdot \mathbf{1} \in H_n$. Moreover, since

$$\|(c + (\vec{u} - \vec{u}_n \cdot \mathbf{1})) - c\|_\infty = \|\vec{u} - \vec{u}_n \cdot \mathbf{1}\|_\infty < \delta,$$

one has $l' \in L_{l_0}$. Thus, there exists $i' \in \llbracket 1, n \rrbracket$ such that $(b_{l'}^I)_{i'} = c_{i'} \leq (c + \vec{u})_{i'}$ and thus $b_{l'}^I \leq_n (c + \vec{u})$ since $b_{l'}^I$ and $c + \vec{u}$ are comparable on the diagonal line l' . Finally, $b_{l'}^I \leq_n c + \vec{u} \leq_n c + \vec{v} <_n b_l^I$, and $R_{b_{l'}^I, b_l^I}$ is not flat, contradicting Lemma 3.9. Hence, $b_l^I \leq_n [c]_l$.

The proof applies straightforwardly to deathpoints by symmetry. \square

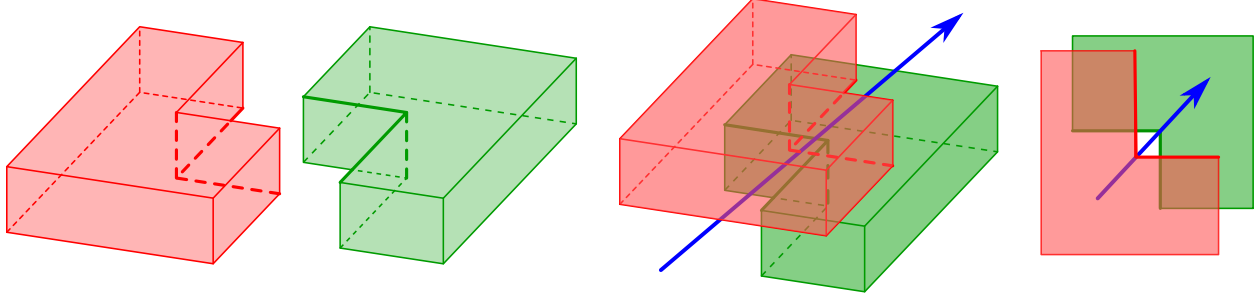


Figure 9: Example of interval module in dimension $n = 3$ with large facets, small holes and some facets with the same codirection close to each other. The support of the module can be constructed by taking the (closed) red and (open) green L -shaped sets on **(Left)**, and glue them together as shown in **(Middle)**. While arbitrarily large facets can be created using this construction, the resulting interval always contains a small hole and large facets of same codirection that are close to each other. Because of this, it is possible to find a (blue) diagonal line that goes through the support without intersecting it, while lines in its surrounding set will detect some facets. **(Right)** View of the interval from the top showing the hole and the spatially close facets (showed in bold font). This is an example where Assumptions 1 and 4 of Definition 4.4 are satisfied, while Assumptions 2 and 3 are not.

Lemma 4.6. *Let $\delta > 0$ and K be a hyperrectangle of \mathbb{R}^n . Let I be a δ -discretely presented interval module in K , and let L be the δ -grid of lines associated to $K^{2\delta}$. Then, there is a bijection between the facets of I and the labels identified by Algorithm 3.*

Proof. We first prove the result for birthpoints and facets of $L[I]$.

Let F be a facet of $L[I]$. Let $l_F \in L$ be a diagonal line intersecting F , and $b_F \in \mathbb{R}^n$ be the associated birthpoint. By Definition 4.4, item (1), there exists an $(n - 1)$ -hypercube $Q_F^{b_F} \subseteq F$ of side length 2δ such that $b_F \in Q_F^{b_F}$. This ensures that for any dimension i that is not in the codirection: $i \in \llbracket 1, n \rrbracket \setminus \text{codir}(F)$, one has either $b_F + \delta e_i \in Q_F^{b_F}$ or $b_F - \delta e_i \in Q_F^{b_F}$. Since L is the δ -grid of lines associated to $K^{2\delta}$, and since $Q_F^{b_F}$ is an $(n - 1)$ -hypercube, there exists a line $l_0 \in L$ such that l_F belongs to the surrounding set L_{l_0} , and such that the birthpoints corresponding to the lines in L_{l_0} are all in $Q_F^{b_F}$. This means that $\text{codir}(F)$ is detected as a label of b_F by Algorithm 3.

Reciprocally, assume there exists a line $l_0 \in L$ such that all birthpoints associated to the lines in the surrounding set L_{l_0} share a coordinate along dimension $i \in \llbracket 1, n \rrbracket$, so that i is a label detected by Algorithm 3. Then, the set of birthpoints $B_{L_{l_0}}$ has a minimal element, and thus its convex hull $\text{conv}(B_{L_{l_0}})$ is in $L[I]$. Since $\text{conv}(B_{L_{l_0}})$ is an $(n - 1)$ -hypercube of codirection i , it must be associated to a facet of $L[I]$ of codirection i as well.

The proof extends straightforwardly for deathpoints. \square

Now that we have proved that all facets can be detected with δ -grids of lines and δ -discretely presented modules, we can state our first main result, which claims that it is possible to *exactly* recover the underlying module under the same assumptions.

Proposition 4.7 (Exact recovery). *Let $\delta > 0$ and $K = R_{\alpha, \beta}$ be a hyperrectangle of \mathbb{R}^n , where $\alpha \leq_n \beta$. Let I be a δ -discretely presented interval module in K , and let L be the δ -grid of lines associated to $K^{2\delta}$. Let $C_B^L(I)$ and $C_D^L(I)$ be the L -birth and death corners of I computed by Algorithm 4, and let $\tilde{I} = \text{Int} \left(\bigcup_{c \in C_B^L(I)} \bigcup_{c' \in C_D^L(I)} R_{c, c'} \right)$ be the approximation computed by Algorithm 2. Then, one has*

$$d_I(I, \tilde{I}) = d_B(I, \tilde{I}) = 0. \quad (10)$$

Proof. As interval modules are characterized by their support, it is enough to show that $\overline{\text{supp}(I)} = \overline{\text{supp}(\tilde{I})}$.

In the following, we thus assume that $\text{supp}(I)$ is closed in $\overline{\mathbb{R}^n}$. We will also use an additional definition. Let b be an infinite corner computed by Algorithm 4. We say that b' is a *pseudo birth corner* for b if:

1. $b'_i = b_i$ for all $i \in \llbracket 1, n \rrbracket \setminus \mathcal{J}$, and for each dimension $j \in \mathcal{J}$, there exists a hyperplane of codirection j intersecting K such that $\bigcap_j H_j \ni b'$. The set \mathcal{J} is called the *codirection* of b' and denoted with $\text{codir}(b')$, and the set $\llbracket 1, n \rrbracket \setminus \mathcal{J}$ is called the *direction* of b' and is denoted with $\text{dir}(b')$.
2. there exists a line $l_0 \in L$ such that
 - (a) $b' \in \text{conv}(L_{l_0}) \cap K^{2\delta} \setminus K$,
 - (b) for each line $l \in L_{l_0}$, the endpoint b'_l is non trivial,
 - (c) for each dimension $j \in \mathcal{J}$, there exists $l_j \in L_{l_0}$ such that $b'_{l_j} \in H_j$.

Note that codirections can be extended to any finite corner (i.e., that is potentially not the pseudo corner of an infinite corner) straightforwardly, and that pseudo death corners can be defined by symmetry. We now prove Proposition 4.7.

We first show the inclusion $\text{supp}(\tilde{I}) \subseteq \text{supp}(I)$. More specifically, we have to prove that the corners computed by Algorithm 4 all belong to $\text{supp}(I)$. A key argument that we will use several times comes from the following lemma, which allows for a local control of the boundary of $\text{supp}(I)$ using the hyperplanes associated to specific corners.

Lemma 4.8. *Let b be a birthpoint (resp. deathpoint) of I in K^δ , and $l_0 \in L$ be the line such that $b \in \text{conv}(L_{l_0})$ (this line exists since L fills K^δ). Then, one has the following:*

1. *for any facet F of $L[I]$ (resp. $U[I]$) containing b , there exists a line $l_F \in L_{l_0}$ such that $b'_{l_F} \in F$ (resp. $d'_{l_F} \in F$).*
2. *for any dimension i , there exists at most one facet of codirection i intersecting the set of birthpoints (resp. deathpoints) $\{b'_l : l \in L_{l_0}\}$ (resp. $\{d'_l : l \in L_{l_0}\}$).*
3. *let $b'_{L_{l_0}}$ (resp. $d'_{L_{l_0}}$) be the finite corner generated by L_{l_0} . Then, one has:*

$$\begin{aligned} \text{conv}(L_{l_0}) \cap L[I] \cap K^{2\delta} &\subseteq \bigcup_{i \in \text{codir}(b')} \{x \in \mathbb{R}^n : x_i = b'_i\} \\ (\text{resp. } \text{conv}(L_{l_0}) \cap U[I] \cap K^{2\delta}) &\subseteq \bigcup_{i \in \text{codir}(d')} \{x \in \mathbb{R}^n : x_i = d'_i\}. \end{aligned}$$

Proof. We only show the result for birthpoints since the arguments for deathpoints are the same. Let $b \in L[I]$ be a birthpoint in K^δ .

Proof of (1). Let F be a facet containing b . According to Definition 4.4, item (1), there exists an $(n-1)$ -hypercube Q_F^b of side length 2δ such that $Q_F^b \subseteq F$ and $b \in Q_F^b$. Since L is a grid, there exists a line $l \in L$ with $d_\infty(b, l) < \delta$ intersecting Q_F^b . Now, since $b \in \text{conv}(L_{l_0})$, one has $d_\infty(l \cap H_F, L_{l_0} \cap H_F) < \delta$, where H_F is the hyperplane containing F ; thus, $l \in L_{l_0}$ (the argument is the same than in the proof of Proposition 3.13, first paragraph).

Proof of (2). By Proposition 3.13, item (2), the birthpoints associated to lines of L_{l_0} are all contained in a ball of radius δ . Thus, the unicity of the facets with given codirection comes straightforwardly from Definition 4.4, item (3).

Proof of (3). Note that the birthpoint b is obviously included in the facets of $L[I]$ that contain it, which is a subset of the facets associated to the birthpoints of the lines in L_{l_0} . Now, as Lemma 4.6 ensures that the birthpoints associated to lines in L_{l_0} are correctly labelled, the corner generated by L_{l_0} must be on the intersection of the facets containing b . This ensures that

$$b \in \bigcup_{i \in \text{codir}(b')} \{x \in \mathbb{R}^n : x_i = b'_i\}.$$

Since these arguments do not depend on $b \in \text{conv}(L_{l_0})$, the result follows. \square

Now that we have Lemma 4.8, we can prove that finite and infinite corners belong to $\text{supp}(I)$. We will prove the results for birth corners, but the arguments for death corners are symmetric.

Finite corners. Let b be a finite birth corner, associated to a set of consecutive lines L_{l_0} for some line $l_0 \in L$. By assumption, each birthpoint b_l^I , for $l \in L_{l_0}$, is nontrivial; and thus any birthpoint in $\text{conv}(L_{l_0})$ is nontrivial as well, using Definition 4.4, item (2). Let $l \in \text{conv}(L_{l_0})$ be the diagonal line passing through b . Using Lemma 4.8, one has:

$$b_l^I \in \text{conv}(L_{l_0}) \cap L[I] \cap K^{2\delta} \subseteq \left(\bigcup_{i \in \text{codir}(b)} \{x \in \mathbb{R}^n : x_i = b_i\} \right) \cap l = \{b\}.$$

Thus $b = b_l^I$ and $b \in \text{supp}(I)$.

Infinite corners. Let b be an infinite birth corner, and let b' be the minimal (w.r.t. \leq_n) pseudo birth corner for b , which is well defined by construction of b (see Algorithm 4). Let L_{l_0} be the associated set of consecutive lines L_{l_0} , for some line $l_0 \in L$. We will show that, if j is a free coordinate of b' , i.e., if $j \in \text{dir}(b')$, then $b'_j < \alpha_j$ (recall that K is the rectangle $R_{\alpha,\beta}$). The reason we want to prove such inequalities is that they directly lead to the result. Indeed, if $b'_j < \alpha_j$ for any $j \in \text{dir}(b')$, then $b' - t \sum_{j \in \text{dir}(b')} e_j$ belongs to $L[I]$ for any $t > 0$, since otherwise the line $\{b' - t \sum_{j \in \text{dir}(b')} e_j : t > 0\}$ would have to intersect a facet $F \subseteq L[I]$ of codirection j for some $j \in \text{dir}(b')$, which would not intersect K , contradicting Definition 4.4, item (4).

Let $j \in \text{dir}(b')$ be a free coordinate. By contradiction, assume that $b'_j \geq \alpha_j$, and let b^j denote the pseudo birth corner generated by $L_{l_0 - \delta e_j}$. In particular, this means that, for any $l \in L_{l_0}$, $l - \delta e_j \in L$ and $L_{l - \delta e_j} \subseteq L$ since L fills K^δ . Now, if for every line $l \in L_{l_0}$ such that $l = l_0 + \vec{v}$ with $\vec{v}_j = 0$, one has that b_l^I and $b_{l - \delta e_j}^I$ are on the same facets, then one has $b_{l - \delta e_j}^I = b_l^I - \delta e_j$, and the pseudo corner b^j is equal to $b' - \delta e_j$ by construction, as per Algorithm 4. Moreover, one has $b^j = b' - \delta e_j \leq_n b'$, contradicting the fact that b' is minimal. Hence, there is at least one line $l \in L_{l_0}$, $l = l_0 + \vec{v}$ with $\vec{v}_j = 0$, such that b_l^I and $b_{l - \delta e_j}^I$ are not on the same facets, in other words, there exists a facet F_j of $L[I]$ of codirection j that intersects the (half-open) segment $[b_l^I - \delta e_j, b_l^I]$. In order to locate that facet more precisely, we will prove the following lemma:

Lemma 4.9. *For any $i \in \llbracket 1, n \rrbracket$ and $s, t \in \mathbb{R}$ such that $s < t$, one has $(b_{l - te_i}^I)_i \leq (b_{l - se_i}^I)_i$.*

Proof. Without loss of generality, assume $s = 0$. Since $b_l^I - te_i \in l - te_i$, it follows that $b_l^I - te_i$ and $b_{l - te_i}^I$ are comparable. Moreover, one must have $b_l^I - te_i \leq_n b_{l - te_i}^I$, otherwise one would have $b_l^I >_n b_l^I - te_i >_n b_{l - te_i}^I$, contradicting Lemma 3.9. If the points are equal, i.e., $b_l^I - te_i = b_{l - te_i}^I$, then one has $(b_l^I)_i \geq (b_{l - te_i}^I)_i$. Otherwise, if $b_l^I - te_i <_n b_{l - te_i}^I$, then

$$\forall k \neq i, (b_{l - te_i}^I)_k > (b_l^I)_k.$$

Moreover, since b_l^I and $b_{l - te_i}^I$ cannot be comparable as per Lemma 3.9 one must have $(b_{l - te_i}^I)_i \leq (b_l^I)_i$. \square

Let $H_j = \{x \in \mathbb{R}^n : x_j = c_j\}$ be the hyperplane associated to F_j . Then, by Lemma 4.9, one has

$$(b_{l-\delta e_j}^I)_j \leq c_j < (b_l^I)_j.$$

Since the lines l and $l - \delta e_j$ both belong to the surrounding set $L_{l_0 - \delta e_j}$, it follows from Lemmas 4.6, and 4.8, item (3), that $\text{codir}(b^j) \supseteq \text{codir}(b') \cup \{j\}$. Moreover, since the facets of $L[I]$ associated to $\text{codir}(b^j)$ are unique in a δ -ball around b^j , as per Definition 4.4, item (3), they all have a unique associated value c_i (corresponding to their associated hyperplanes).

Finally, we will show that $b^j \leq_n b'$. Let $i \in \llbracket 1, n \rrbracket$ be an arbitrary dimension.

- If $i \in \text{codir}(b')$, then $b_i^j = b'_i$.
- If $i \in \text{codir}(b^j) \setminus \text{codir}(b')$, then $b_i^j \in \left\{ c_i, \min_{l \in L_{l_0 - \delta e_j}} (b_l^I)_i \right\} \leq \min_{l \in L_{l_0}} (b_l^I)_i = b'_i$, with a strict inequality for $i = j$.
- If $i \in \text{dir}(b^j) \subseteq \text{dir}(b')$, then $b_i^j = \min_{l \in L_{l_0 - \delta e_j}} (b_l^I)_i \leq \min_{l \in L_{l_0}} (b_l^I)_i = b'_i$.

Hence, one always has $b_i^j \leq b'_i$, and thus $b^j <_n b'$, which contradicts the fact that b' is minimal. Thus, one must have $b'_j < \alpha_j$.

We now show that $\text{supp}(I) \subseteq \text{supp}(\tilde{I})$. Let $x \in \text{supp}(I)$. We will show that there exists a birth corner c such that $c \leq_n x$. Let \mathcal{H} be the family of hyperplanes associated to the facets of $L[I]$. The corner c will be defined as the limit of a sequence of points $\{x^{(k)}\}_{k \in \mathbb{N}^*}$ in $\overline{\mathbb{R}}^n$, defined by induction with:

1. $x^{(1)} = \inf \{x - t \cdot \mathbf{1} : t \geq 0\} \cap \text{supp}(I)$. Then, one has the two following possibilities:
 - either $x^{(1)} = -\infty$, and we let $c := x^{(1)}$.
 - or there exists a maximal subset of hyperplanes $\mathcal{H}^1 \subset \mathcal{H}$, $\mathcal{H}^1 \neq \emptyset$, such that $x^{(1)} \in \bigcap_{H \in \mathcal{H}^1} H =: H_1$. Let $\mathcal{J}^1 \subseteq \llbracket 1, n \rrbracket$ be the set of free coordinates in H_1 , i.e., those dimensions such that $j \in \mathcal{J}^1 \iff x^{(1)} - e_j \in H_1$.
2. $x^{(2)} = \inf \left\{ x^{(1)} - t \cdot \sum_{j \in \mathcal{J}^1} e_j : t \geq 0 \right\} \cap \text{supp}(I)$. Then, one has the two following possibilities:
 - either $x^{(2)}$ is at infinity in H_1 , i.e., $x_j^{(2)} = -\infty$ if $j \in \mathcal{J}^1$ and $x_j^{(2)} = x_j^{(1)}$ otherwise, and we let $c := x^{(2)}$.
 - or there exists a maximal subset of hyperplanes $\mathcal{H}^2 \supsetneq \mathcal{H}^1$ such that $x^{(2)} \in \bigcap_{H \in \mathcal{H}^2} H =: H_2$. Let $\mathcal{J}^2 \subseteq \llbracket 1, n \rrbracket$ be the set of free coordinates in H_2 , i.e., those dimensions such that $j \in \mathcal{J}^2 \iff x^{(2)} - e_j \in H_2$.
3. For $k \geq 3$, $x^{(k+1)} = \inf \left\{ x^{(k)} - t \cdot \sum_{j \in \mathcal{J}^k} e_j : t \geq 0 \right\} \cap \text{supp}(I)$. Then, one has the two following possibilities:
 - either $x^{(k+1)}$ is at infinity in H_k , i.e., $x_j^{(k+1)} = -\infty$ if $j \in \mathcal{J}^k$ and $x_j^{(k+1)} = x_j^{(k)}$ otherwise, and we let $c := x^{(k+1)}$.
 - or there exists a maximal subset of hyperplanes $\mathcal{H}^{k+1} \supsetneq \mathcal{H}^k$ such that $x^{(k+1)} \in \bigcap_{H \in \mathcal{H}^{k+1}} H =: H_{k+1}$. Let $\mathcal{J}^{k+1} \subseteq \llbracket 1, n \rrbracket$ be the set of free coordinates in H_{k+1} , i.e., those dimensions such that $j \in \mathcal{J}^{k+1} \iff x^{(k+1)} - e_j \in H_{k+1}$.

If this sequence stops at step one, i.e., $c = x^{(1)} = -\infty$, then every birthpoint of I is at $-\infty$, the only birth corner is $c = -\infty$, and one trivially has $c \leq_n x$. Hence, we assume in the following that c is obtained after at least one iteration of the sequence. Note that this sequence of points has length at most n . Let

c^- and c be the penultimate and last elements of the sequence respectively, and let \mathcal{J}^- be the set of free coordinates associated to c^- . By construction, one has:

$$c \leq_n c^- \leq_n \cdots \leq_n x^{(2)} \leq_n x^{(1)} \leq_n x.$$

We now show that c is indeed a birth corner. If c is finite, then it must belong to the intersection of n hyperplanes, and it is thus a finite birth corner. Hence, we assume now that c is not finite. We will construct a minimal pseudo birth corner from c^- , and show that c is its associated infinite birth corner. We will consider two different cases, depending on whether c^- is close to $K = R_{\alpha, \beta}$ or not. If $c^- \in K^\delta$, the filling property of L and the size of the facets of $L[I]$ ensure that c^- is itself a minimal pseudo birth corner, associated to c , which is thus an infinite birth corner. If $c^- \notin K^\delta$, then let $\vec{v} \in \mathbb{R}^n$ be a vector that pushes back c^- into K^δ , i.e., such that, for any dimension $i \in \mathcal{J}^-$, one has

$$\alpha_i - \delta \leq (c^- + \vec{v})_i < \alpha_i,$$

and $\vec{v}_i = 0$ if $i \notin \mathcal{J}^-$. Let S be the segment $[c^-, c^- + \vec{v}]$. We have the two following cases:

1. Assume $S \subseteq L[I]$. Then $c^- + \vec{v} \in \text{supp}(I) \cap K^\delta$, and there exists a line $l \in L$ such that $c^- + \vec{v} \in \text{conv}(L_l)$. Let c^l be the pseudo birth corner associated to L_l . Since one has $c_j^l < \alpha_j$ for any dimension $j \in \mathcal{J}^-$, it follows that $\mathcal{J}^- \subseteq \text{dir}(c^l)$. Furthermore, since $c^- + \vec{v}$ belongs to the same facets than c and c^- , and since $c^- + \vec{v} \in \text{conv}(L_l)$ one has $\text{codir}(c^l) \supseteq \text{codir}(c)$ and $\text{dir}(c) = \mathcal{J}^-$. Thus, c is an infinite birth corner associated to the minimal pseudo birth corner c^l .
2. Assume $S \not\subseteq L[I]$. In that case, there must be a facet of codirection j , for some $j \in \mathcal{J}^-$, that intersects S . Since one has $c_j^- \leq (c^- + \vec{v})_j < \alpha_j$ for any $j \in \mathcal{J}^-$, this means that the facet would not intersect K , which yields to a contradiction as per Definition 4.4, item (4).

This concludes that $\text{supp}(I) \subseteq \text{supp}(\tilde{I})$, and the equality between these supports holds. \square

Proposition 4.7 extends to the following corollary, whose proof is immediate from the definition of exact matchings (see Definition 3.1 above).

Corollary 4.10. *Let \mathbb{M} be an interval decomposable multi-parameter persistence module, whose interval summands all satisfy the assumptions of Proposition 4.7. Let $\tilde{\mathbb{M}}_\delta^{\text{MMA}} := \text{MMA}(\mathbb{M}, L_\delta(K^{2\delta}), \sigma)$ be the multi-parameter persistence module computed by MMA. Then, one has*

$$d_I(\mathbb{M}, \tilde{\mathbb{M}}_\delta^{\text{MMA}}) = d_B(\mathbb{M}, \tilde{\mathbb{M}}_\delta^{\text{MMA}}) = 0.$$

4.4 Stability properties of MMA

In the previous sections, we have seen that MMA provides candidate decompositions that approximate well, and sometimes exactly, the interval decomposition of the true underlying module, when it exists. In this section, we focus on the general case, when \mathbb{M} does not decompose into simple summands, so that there is no clear notion of induced matching $\sigma_{\mathbb{M}}$. In this case, using matching functions that pair bars that are *compatible* still preserves structural properties of \mathbb{M} with MMA. Thus we start by defining compatibility.

Definition 4.11 (Compatible bars). *Let \mathbb{M} be a multi-parameter persistence module, and let $l_1, l_2 \subseteq \mathbb{R}^n$ be two diagonal lines that are at distance δ from each other. Assume $\text{supp}(\mathbb{M}) \cap l_1$ and $\text{supp}(\mathbb{M}) \cap l_2$ are not empty, and let $[b_{l_1}^{\mathbb{M}}, d_{l_1}^{\mathbb{M}}]$ and $[b_{l_2}^{\mathbb{M}}, d_{l_2}^{\mathbb{M}}]$ be bars in $\mathcal{B}(\mathbb{M}|_{l_1})$ and $\mathcal{B}(\mathbb{M}|_{l_2})$, characterized by their endpoints. These bars are compatible if the rectangles $R_{b_{l_1}^{\mathbb{M}}, b_{l_2}^{\mathbb{M}}}$, $R_{b_{l_2}^{\mathbb{M}}, b_{l_1}^{\mathbb{M}}}$, $R_{d_{l_1}^{\mathbb{M}}, d_{l_2}^{\mathbb{M}}}$ and $R_{d_{l_2}^{\mathbb{M}}, d_{l_1}^{\mathbb{M}}}$ are flat. Moreover, we say that $[b_{l_1}^{\mathbb{M}}, d_{l_1}^{\mathbb{M}}]$ is compatible with the empty set in l_2 if $\|b_{l_1}^{\mathbb{M}} - d_{l_1}^{\mathbb{M}}\|_\infty \leq 2\delta$.*

A compatible matching function is a matching function that only pairs bars that are compatible.

Note that the vineyards algorithm provides compatible matching functions when δ is small enough (see Section 5.2). The main motivation for using compatible matching functions is that the candidate decompositions they induce with MMA preserve the barcodes on *any* diagonal line intersecting K up to 2δ .

Proposition 4.12. *Let \mathbb{M} be a multi-parameter persistence module. Let σ be a compatible matching function for $\mathcal{FB}(\mathbb{M})_L$, and let $\tilde{\mathbb{M}}_\delta^{\text{MMA}} := \text{MMA}(\mathbb{M}, L_\delta(K^\delta), \sigma)$. Let l be a diagonal line intersecting K . Then, one has $d_B(\mathcal{B}(\mathbb{M}|_l), \mathcal{B}(\tilde{\mathbb{M}}|_l)) = 0$ if $l \in L$, and $d_B(\mathcal{B}(\mathbb{M}|_l), \mathcal{B}(\tilde{\mathbb{M}}|_l)) \leq 2\delta$ otherwise.*

Proof. Since the proof of Proposition 4.3 above is based on repeated applications of Lemma 3.9, the exact same arguments can be used to prove the first part of Proposition 4.12 (the fact that MMA with compatible matchings provides δ -candidate decompositions, i.e., preserve exactly the L -fibered barcodes). Indeed, compatible matchings also guarantee (by definition) the flatness of rectangles created by consecutive endpoints. The general upper bound for any diagonal line is then a simple consequence of Lemma 3.10. Indeed, given a line $l \notin L$, there must be a line $l^* \in L$ such that $l^* = l + \vec{u}$ with $\|\vec{u}\| \leq \delta$ since L fills K . Then, one has $d_B(\mathcal{B}(\mathbb{M}|_l), \mathcal{B}(\tilde{\mathbb{M}}|_l)) \leq d_B(\mathcal{B}(\mathbb{M}|_l), \mathcal{B}(\mathbb{M}|_{l^*})) + d_B(\mathcal{B}(\mathbb{M}|_{l^*}), \mathcal{B}(\tilde{\mathbb{M}}|_{l^*})) + d_B(\mathcal{B}(\tilde{\mathbb{M}}|_{l^*}), \mathcal{B}(\tilde{\mathbb{M}}|_l)) \leq \delta + 0 + \delta = 2\delta$ by Lemma 3.10. \square

While this result is weaker than preserving the rank invariant (which would require controlling the barcodes of all lines with positive slopes), preserving the barcodes of all diagonal lines is still a nice guarantee that ensures that the candidate decompositions provided by MMA are still appropriate, stable invariants in the general case when computed with compatible matchings. Note also that if \mathbb{M} is interval decomposable, then compatible matchings commute with the induced matching $\sigma_{\mathbb{M}}$ under specific conditions (see Section 5.1), and can thus also be used for applying Proposition 3.4.

However, it is not possible to control more powerful distances such as d_I (see Section 4.5), which is expected when building visual, interpretable invariants from modules that do not decompose simply. Hence, we end this section by ensuring that MMA can still remain stable w.r.t. to the data itself by appropriately choosing the matching functions. Indeed, given two multi-parameter filtrations computed from the sublevel sets of functions f, g , Equation (1) ensures that the bottleneck distances between barcodes in the fibered barcodes of $\mathbb{M}(f)$ and $\mathbb{M}(g)$ are upper bounded by $\|f - g\|_\infty$. This in turns means that we can fix an (arbitrary) matching function σ_f for computing a candidate decomposition of f with MMA, and define another one σ_g that commutes with σ_f and the optimal partial matching ν given by those bottleneck distances. Doing so leads to the following proposition.

Proposition 4.13. *Let $f, g : S \rightarrow \mathbb{R}^n$ be two continuous functions defined on a simplicial complex S . Let K be a hyperrectangle containing the minimal Betti numbers of $\mathbb{M}(f)$ and $\mathbb{M}(g)$. Let σ_f be an arbitrary matching function. Then, there exists a matching function σ_g , and corresponding candidates $\tilde{\mathbb{M}}_\delta^{\text{MMA}}(f) := \text{MMA}(\mathbb{M}(f), L_\delta(K^\delta), \sigma_f)$ and $\tilde{\mathbb{M}}_\delta^{\text{MMA}}(g) := \text{MMA}(\mathbb{M}(g), L_\delta(K^\delta), \sigma_g)$ such that:*

$$d_I(\tilde{\mathbb{M}}_\delta^{\text{MMA}}(f), \tilde{\mathbb{M}}_\delta^{\text{MMA}}(g)) \leq d_B(\tilde{\mathbb{M}}_\delta^{\text{MMA}}(f), \tilde{\mathbb{M}}_\delta^{\text{MMA}}(g)) \leq \|f - g\|_\infty + \delta.$$

Proof. Let σ_g be the matching function induced by the following commutative diagram:

$$\begin{array}{ccc} \mathcal{B}(\mathbb{M}(f)|_l) & \xrightarrow{\sigma_f} & \mathcal{B}(\mathbb{M}(f)|_{l'}) \\ \downarrow \nu_{l, d_B} & & \downarrow \nu_{l', d_B} \\ \mathcal{B}(\mathbb{M}(g)|_l) & \xrightarrow{\sigma_g} & \mathcal{B}(\mathbb{M}(g)|_{l'}) \end{array}$$

where ν_{l, d_B} denotes the optimal partial matching induced by $d_B(\mathcal{B}(\mathbb{M}(f)|_l), \mathcal{B}(\mathbb{M}(g)|_l))$.

Let I_f, I_g denote two interval summands of $\tilde{\mathbb{M}}_\delta^{\text{MMA}}(f)$ and $\tilde{\mathbb{M}}_\delta^{\text{MMA}}(g)$ that are paired by ν_{l, d_B} . Then, controlling the bottleneck distance between these outputs of MMA simply amounts to controlling the Hausdorff distance between $\text{supp}(I_f)$ and $\text{supp}(I_g)$. In order to control this distance, let B_f and B_g denote the bars that induced these interval summands as per Algorithm 2. Then, one has $B_f \subseteq \text{supp}(I_f)$ and $B_g \subseteq B_f^\gamma$, where $\gamma = \|f - g\|_\infty$. Thus, since $\text{supp}(I_g) \subseteq B_g^\delta$ (by construction), one has $\text{supp}(I_g) \subseteq B_f^{\gamma+\delta} \subseteq \text{supp}(I_f)^{\gamma+\delta}$. The result follows by symmetry of f and g . \square

4.5 Instability of MMA w.r.t. interleaving distance

While using compatible matchings helps controlling the L -fibered barcodes, it is unfortunately not sufficient for bounding the interleaving distance: outputs of **MMA** can be very far in terms of d_I while the modules they are computed from are not. We provide two multi-parameter persistence modules in Figure 10 that illustrate such lack of stability. In this figure, the two bi-filtrations only differ on the middle edge (in blue) of the simplicial complex. When the appearance of this edge is delayed (as is the case for the multi-parameter filtration displayed on top), the bars in the barcodes corresponding to the lower and upper cycles of the simplicial complex get paired with the compatible matching, and create together the large red summand. On the other hand, this does not happen for the other multi-parameter filtration: the bars corresponding to these cycles are never paired and form distinct summands with same size.

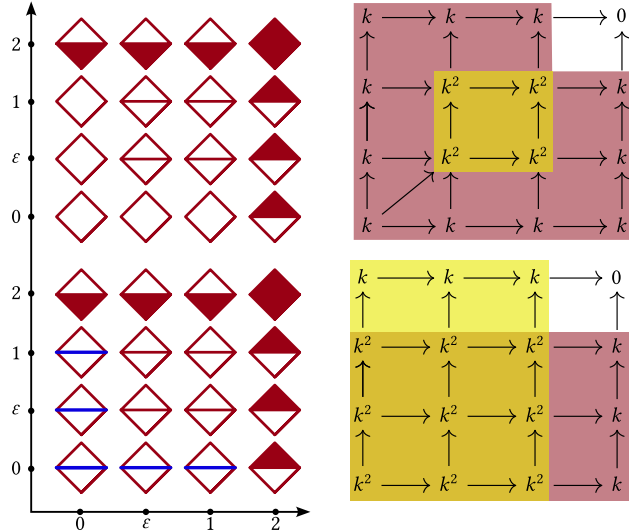


Figure 10: **(Left)** Two bi-filtrations whose corresponding multi-parameter persistence modules in homology dimension 1 are ϵ -interleaved. **(Right)** The two corresponding, significantly different interval decompositions obtained with **MMA** computed with a compatible matching. Intervals in these decompositions are displayed with red and yellow colors.

Figure 10 illustrates the price to pay for designing interpretable decompositions (i.e., such that each summand corresponds to a cycle of the simplicial complex) when several choices are possible: there are several different ways to assign cycles to summands in the non-interval decomposable module displayed on top of Figure 10—the one computed by **MMA** (shown in the figure) being one possibility. An important conjecture of this article, that is left for future work, is that stacking the candidate decompositions produced by **MMA** for all possible matching functions induces a complete invariant.

5 Matching functions for MMA

In this section, we study general properties of matching functions that can be used as inputs for **MMA**. One might wonder whether the usual distances between barcodes, such as the bottleneck or Wasserstein distances, could be used to define exact matching functions. Indeed, a major advantage of, e.g., Wasserstein distances, is that their associated matching functions are usually unique. However, when the space δ between two lines is too large, Wasserstein distances can still fail to match bars exactly, as shown in Figure 11.

We show in Section 5.1 that matching functions that are compatible (see Definition 4.11) commute with the matching functions induced by interval decomposable modules. Then, we discuss matching functions induced by the vineyards algorithm in Section 5.2.

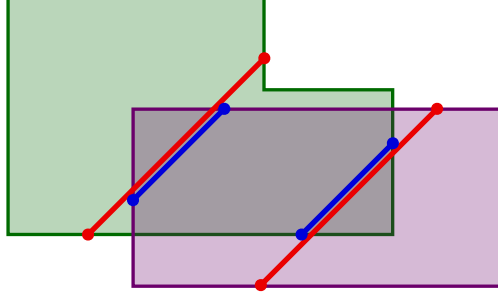


Figure 11: Example interval decomposable multi-parameter persistence module with two interval summands (green and purple), and its barcodes along two lines (here the two couples of red-blue bars). Any matching function induced by, e.g., Wasserstein distances between the barcodes, will match the first red bar with the second red bar and the first blue bar with the second blue bar; however, this matching is not exact.

5.1 Compatible matching functions

In this section, we show that compatible matching functions commute with the induced matching function $\sigma_{\mathbb{M}}$ (when \mathbb{M} is interval decomposable) under some specific conditions. In the rest of this section, given a matching function σ that commutes with $\sigma_{\mathbb{M}}$, we will also call σ *exact* for the sake of simplicity. Before stating the main result, we first show a technical lemma that relates the locations of endpoints of compatible bars with each other.

Lemma 5.1. *Let l_1 and l_2 be two δ -consecutive lines, and let $[b_1, d_1] := \mathcal{B}(I|_{l_1})$ be the bar of an interval module along l_1 . Let $[b_2, d_2]$ be a bar along l_2 that is compatible with $[b_1, d_1]$. Then, d_2 (resp. b_2) is included in a segment of size δ in l_2 .*

Proof. Applying Lemma 3.10, one has

$$d_2 \in C := [B_\delta(d_1) \cap l_2] \setminus [\{z \in \mathbb{R}^n : z > d_1\} \cup \{z \in \mathbb{R}^n : z < d_1\}]$$

Since C is a nonempty, totally ordered set, we can define $y := \min C$. By construction, there exists a dimension i such that $y_i \geq (d_1)_i$, and thus C must be included in the segment $[y, y + \delta \cdot \mathbf{1}]$ along l_2 .

The proof applies straightforwardly to b_2 by symmetry. \square

Since bars that are matched under an exact matching function are always compatible, one way to construct an exact matching function between two barcodes is therefore to isolate, among all possible matching functions, the ones such that matched bars are compatible. If this family contains a single element, it must be the exact matching we are looking for. This typically happens for interval decomposable multi-parameter persistence module whose summands are sufficiently separated, as we show in the proposition below.

Proposition 5.2. *Let $\mathbb{M} = \bigoplus_{I \in \mathcal{I}} I$ be an interval decomposable multi-parameter persistence module. Let $\delta > 0$, and I, I' be two interval summands in the decomposition of \mathbb{M} . Assume that the two following properties are satisfied:*

1. *Let $l \subset \mathbb{R}^n$ be a diagonal line such that $\text{supp}(I) \cap l \neq \emptyset$ and $\text{supp}(I') \cap l \neq \emptyset$. Then, one has either $\|b_l^I - b_l^{I'}\|_\infty > \delta$ or $\|d_l^I - d_l^{I'}\|_\infty > \delta$. In other words, the endpoints of the bar in $\mathcal{B}(I|_l)$ and of the bar in $\mathcal{B}(I'|_l)$ are at distance at least δ .*
2. *The bars of length at most 2δ in I and I' are at distance at least δ , i.e., if we let*

$$S^I := \{l : l \cap \text{supp}(I) \neq \emptyset, \|b_l^I - d_l^I\|_\infty \leq 2\delta\},$$

(and similarly for I'), one has $d_\infty(S^I, S^{I'}) > \delta/2$. In other words, a small bar in I cannot be too close to a small bar in I' .

Then, the matching function σ_{comp} , induced by matching bars that are compatible together, is well-defined and exact.

See Figure 12 for an illustration of assumptions (1) and (2).

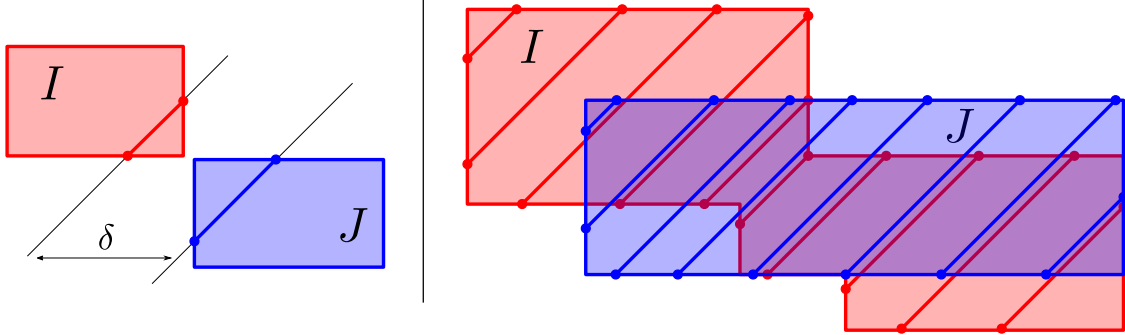


Figure 12: **(Left)** Example of module whose interval summands do not satisfy assumption (2). **(Right)** Example of module whose interval summands do satisfy assumptions (1) and (2). Bars corresponding to consecutive lines can only be matched if they are compatible, which, in this figure, means that they have the same color, i.e., that they are associated to the same interval summand.

Proof. Let I and I' be two interval summands in the decomposition of \mathbb{M} . Let l_1 and l_2 be two δ -consecutive lines of L , and let $b := \mathcal{B}(I|_{l_1})$ be the bar corresponding to I along l_1 . We will show that σ_{comp} must match b to either $b' := \mathcal{B}(I'|_{l_2})$ if $\text{supp}(I) \cap l_2 \neq \emptyset$, or the empty set if $\text{supp}(I) \cap l_2 = \emptyset$.

- If $\text{supp}(I) \cap l_2 = \emptyset$, then by Lemma 3.10, the length of b is at most δ , i.e., $\|b_{l_1}^I - d_{l_1}^I\|_\infty \leq \delta$. It is thus compatible with the empty set. Now, since $d_\infty(l_1, l_2) = \delta/2$ and since $l_1 \in S^I$, assumption (2) ensures that the bar $b'' := \mathcal{B}(I'|_{l_2})$ (if it exists) must be of length at least 2δ . In particular, it is not compatible with b , hence σ_{comp} cannot match b to b'' , and must match b to the empty set.
- If $\text{supp}(I) \cap l_2 \neq \emptyset$, then the bar $b' = [b_{l_2}^I, d_{l_2}^I]$ in $\mathcal{B}(I|_{l_2})$ is compatible with b , as per Lemma 3.9. According to Lemma 5.1, it follows that the birthpoint and deathpoint of any bar along l_2 that is compatible to l_1 must belong to segments s_b, s_d of length δ that contain $b_{l_2}^I$ and $d_{l_2}^I$ respectively. Let $b'' := [b_{l_2}^{I'}, d_{l_2}^{I'}]$ be the bar in $\mathcal{B}(I'|_{l_2})$ (if it exists). According to assumption (1), we either have $\|b_{l_2}^I - b_{l_2}^{I'}\|_\infty > \delta$ or $\|d_{l_2}^I - d_{l_2}^{I'}\|_\infty > \delta$. In particular this means that either $b_{l_2}^{I'} \notin s_b$ or $d_{l_2}^{I'} \notin s_d$. Hence b'' is not compatible with b , and σ_{comp} must match b to b' .

In both cases, σ_{comp} is well-defined and exact. □

5.2 Vineyards matching functions

This section is dedicated to the vineyards algorithm for simplicial complexes. It is quite technical and can be skipped by readers who are most interested in the general exposition. The vineyards algorithm provides a matching function σ_{vine} between barcodes, so the purpose of this section is to show that it is exact, i.e., that it commutes with the induced matching function $\sigma_{\mathbb{M}}$, provided that \mathbb{M} is interval decomposable. Since vineyards are heavily based on simplicial homology, we first recall the basics of persistent homology from simplicial complexes in Section 5.2.1. Then, we provide an analysis of the vineyards algorithm in Section 5.2.2.

5.2.1 Persistent homology of simplicial complexes

We assume in the following that the reader is familiar with simplicial complexes, boundary operators and homology groups, and we refer the interested reader to [Mun84, Chapter 1] for a thorough treatment of these notions. The first important definition is the one of *filtered simplicial chain complexes*.

Definition 5.3. *Let S be a simplicial complex, and $f: S \rightarrow \mathbb{R}$ be a filtration function, i.e., f satisfies $f(\sigma) \leq f(\tau)$ when $\sigma \subseteq \tau$. Then, the filtered simplicial chain complex (S, f) is defined as $(S, f) = ((C_t)_{t \in \mathbb{R}}, \iota)$, where*

- $C_t = \langle \sigma_0, \dots, \sigma_i \rangle$ is the vector space over a field k whose basis elements are the simplices that have filtration values smaller than t , i.e., $\{\sigma_0, \dots, \sigma_i\} = \{\sigma \in S : f(\sigma) \leq t\}$, and
- for any $s \leq t$, the map $\iota = \iota_s^t: C_s \hookrightarrow C_t$ is the canonical injection.

Note that f can be used to define an order on the simplices of $S = \{\sigma_i\}_{i=0}^N$, by using the ordering induced by the filtration values. In other words, we assume in the following that $f(\sigma_0) \leq f(\sigma_1) \leq \dots \leq f(\sigma_N)$. We also slightly abuse notations and define $C_i := \langle \sigma_0, \dots, \sigma_i \rangle$ for any $i \in \llbracket 0, N \rrbracket$ and

$$(S, f) = \left(C_0 \xrightarrow{\iota_0} C_1 \xrightarrow{\iota_1} \dots \xrightarrow{\iota_{N-1}} C_N = \langle S \rangle \right). \quad (11)$$

Then, applying the homology functor H_* on this filtered simplicial chain complex yields the following (single-parameter) persistence module

$$H_*(S, f) = 0 \rightarrow H_*(C_0) \rightarrow H_*(C_1) \rightarrow \dots \rightarrow H_*(C_N).$$

An important theorem of single-parameter persistent homology states that, up to a change of basis, it is possible to pair some chains together in order to define the so-called *one-dimensional persistence barcode* associated to the filtered simplicial chain complex.

Theorem 5.4 (Persistence pairing, [dMV11, Theorem 2.6]). *Given a filtered simplicial chain complex $(S, f) = C_1 \hookrightarrow C_2 \hookrightarrow \dots \hookrightarrow C_N$ and associated persistence module $H_*(S, f)$, there exists a partition $\llbracket 1, N \rrbracket = E \sqcup B \sqcup D$, a bijective map $\text{Low} : D \rightarrow B$, and a new basis $\hat{\sigma}_1, \dots, \hat{\sigma}_N$ of C , called reduced basis, such that:*

- $C_i = \langle \hat{\sigma}_1, \dots, \hat{\sigma}_i \rangle$,
- $\partial \hat{\sigma}_e = 0$ for any $e \in E$,
- for any $d \in D$, one has $\partial \hat{\sigma}_{\text{Low}(d)} = 0$, and $\partial \hat{\sigma}_d$ is equal to $\hat{\sigma}_{\text{Low}(d)}$ up to simplification, i.e., there exists a set of indices $\text{bd}(d)$ such that (i) $j < \text{Low}(d) \leq d$ for any $j \in \text{bd}(d)$, and (ii) $\partial \hat{\sigma}_d = \hat{\sigma}_{\text{Low}(d)} + \sum_{j \in \text{bd}(d)} \hat{\sigma}_j$.

In particular, the chains $\{\hat{\sigma}_j : j \in E \cap \llbracket 1, i \rrbracket\} \cup \{\hat{\sigma}_j : j \in B \cap \llbracket 1, i \rrbracket\}$ and $\exists d > i$ s.t. $\text{Low}(d) = j$ form a basis of the simplicial homology groups $H_*(C_i)$. Moreover, the chains $\{\hat{\sigma}_j : j \in B \sqcup E\}$ are called positive chains while the chains $\{\hat{\sigma}_j : j \in D\}$ are called negative chains.

The multiset of bars $\mathcal{B}(f) := \{[f(\hat{\sigma}_b), f(\hat{\sigma}_d)] : b = \text{Low}(d)\} \cup \{[f(\hat{\sigma}_e), +\infty) : e \in E\}$ is called the persistence barcode of the filtered simplicial chain complex (S, f) and of the single-parameter persistence module $H_*(S, f)$.

Note that while the reduced basis $\{\hat{\sigma}_1, \dots, \hat{\sigma}_N\}$ does not need to be unique, the pairing map Low is actually independent of that reduced basis (see [EH10, VII.1, Pairing Lemma]).

5.2.2 Vineyards algorithm and matching

The vineyards algorithm is a method that allows to find reduced chain bases for filtered simplicial complexes whose simplex orderings only differ by a single transposition of consecutive simplices, that we denote by $(i \ i + 1)$.

Proposition 5.5 ([CSEM06]). *Let $S = \{\sigma_1, \dots, \sigma_N\}$ be a (filtered) simplicial complex (with filtration function f), and let $B = \{\hat{\sigma}_1, \dots, \hat{\sigma}_N\}$ be a corresponding reduced chain basis. Let $\tilde{f} : S \rightarrow \mathbb{R}$ be a filtration function that swaps the simplices at positions i and $i + 1$, i.e., that induces a new filtered simplicial complex $\tilde{S} = \{\sigma_1, \dots, \sigma_{i+1}, \sigma_i, \dots, \sigma_N\}$. Note that the swapped basis $\text{sw}_i^S(B) := \{\hat{\sigma}_1, \dots, \hat{\sigma}_{i+1}, \hat{\sigma}_i, \dots, \hat{\sigma}_N\}$ might not be a reduced basis for (\tilde{S}, \tilde{f}) , since the pairing map Low might not be well-defined anymore. Fortunately, there exists a change of basis, called vineyard update, that turns $\text{sw}_i^S(B)$ into a reduced basis \tilde{B} of (\tilde{S}, \tilde{f}) in $O(N)$ time, and that comes with a bijective map $\sigma_{\text{vine}} : B \rightarrow \tilde{B}$, called vineyard matching, that can be used to define a matching $\sigma_{\text{vine}} : \mathcal{B}(f) \rightarrow \mathcal{B}(\tilde{f})$.*

Note that the vineyards matching can be straightforwardly extended to filtration functions whose induced ordering differs by a whole permutation from the one of the initial filtration function by simply decomposing the permutation into elementary transpositions (using, e.g., Coxeter decompositions).

Application to multi-parameter persistent homology. When the simplices of S are (partially) ordered from a function $f : S \rightarrow \mathbb{R}^n$, i.e., one has $f(\tau) \leq_n f(\sigma)$ for any $\tau \subseteq \sigma$, then the function f is called a *multi-parameter filtration function* of S . In that case, applying the homology functor also leads to simplicial homology groups $\{H_d(C_i)\}_{i \in I}$, where $I \subseteq \llbracket 1, N \rrbracket^n$ is the (partial) ordering associated to f , and these groups are connected by morphisms as long as their indices are comparable in \mathbb{R}^n . These groups and maps are called the *multi-parameter persistent homology* associated to the multi-filtered simplicial chain complex (S, f) . Similarly to the single-parameter case, when k is a field, one can define the *multi-parameter persistence module* \mathbb{M} associated to (S, f) as the family of vector spaces indexed over \mathbb{R}^n defined with the identifications $M_s := H_d(C)$ where $C = \text{Vect}\{\sigma \in S : f(\sigma) \leq s \in \mathbb{R}^n\}$.

We now show that the vineyards algorithm yields an exact matching function, in the sense that it commutes with the exact matching function induced by the underlying module \mathbb{M} when it is interval decomposable.

Proposition 5.6. *Let \mathbb{M} be an interval decomposable multi-parameter persistence module computed from a finite multi-filtered simplicial chain complex (S, f) over \mathbb{R}^n . Then, for a small enough $\delta > 0$, σ_{vine} is exact.*

Proof. Let $\delta > 0$ be such that, for any two lines $l, l' \in L$, there exists a sequence $l = l_1, \dots, l_k = l'$ such that the simplex orderings induced by l_i and l_{i+1} differ by at most one transposition of two consecutive simplices, for any $i \in \llbracket 1, k - 1 \rrbracket$.

Let l, l' be two diagonal lines in \mathbb{R}^n , and let $F := f|_l : S \rightarrow \mathbb{R}$ and $F' := f|_{l'} : S \rightarrow \mathbb{R}$. Up to a reordering of the simplices of $S = \{\sigma_1, \dots, \sigma_N\}$, we assume without loss of generality that $F(\sigma_1) \leq \dots \leq F(\sigma_N)$. Let $\mathfrak{S}_N^S \subseteq \mathfrak{S}_N$ be the subset of permutations that satisfies $\tau \in \mathfrak{S}_N^S \implies (C_k^\tau)_{k \in \llbracket 1, N \rrbracket} = (\{\sigma_{\tau(1)}, \dots, \sigma_{\tau(k)}\})_{k \in \llbracket 1, N \rrbracket}$ is a filtration of S . Finally, let $N = (N_{\tau, k})_{(\tau, k) \in \mathfrak{S}_N^S \times \llbracket 1, N \rrbracket}$, where $N_{\tau, k} = H_*(C_k^\tau)$ is the multi-parameter persistence module indexed over $\mathfrak{S}_N^S \times \llbracket 1, N \rrbracket$, with arrows induced by inclusion. Note that the one-dimensional persistence module $N_{\text{id}} := (N_{\text{id}, k})_{k \in \llbracket 1, N \rrbracket}$ is isomorphic to $\mathbb{M}|_l$.

Now, let τ be the simplex permutation that matches the simplex ordering induced by F to the one induced by F' . By definition, one has $\tau \in \mathfrak{S}_N^S$. Let i be the index of the first transposition, i.e., the transposition $(i \ i + 1)$ given by the reordering of the simplices from $l = l_1$ to l_2 . Then, the matching σ_{vine}^i associated to the transposition $(i \ i + 1)$ induces a matching between the bars of $\mathcal{B}(\mathbb{M}|_l)$ and $\mathcal{B}(\mathbb{M}|_{l_2})$, or equivalently, between the bars of $\mathcal{B}(N_{\text{id}})$ and $\mathcal{B}(N_{(i \ i + 1)})$, as well as a morphism between N_{id} and $N_{(i \ i + 1)}$. Let us now consider the diamond:

$$\begin{array}{ccccc}
 & & N_{(i \ i + 1), i} & & \\
 & \nearrow & & \searrow & \\
 \dots & \longrightarrow & N_{\text{id}, i-1} = N_{(i \ i + 1), i-1} & & N_{\text{id}, i+1} = N_{(i \ i + 1), i+1} \longrightarrow \dots \\
 & \searrow & & \nearrow & \\
 & & N_{\text{id}, i} & &
 \end{array} \tag{12}$$

First, note that all maps in that diamond are either injective of corank 1 or surjective of nullity 1 (since they are all induced by adding a positive or negative chain of the corresponding reduced bases). Moreover, by the Mayer-Vietoris theorem, the following sequence is exact:

$$\begin{aligned} N_{\text{id},i-1} = N_{(i+1),i-1} = H_*(C_{i-1}^{\text{id}}) &\rightarrow N_{(i+1),i} \oplus N_{\text{id},i} = H_*(C_i^{(i+1)}) \oplus H_*(C_i^{\text{id}}) \\ &\xrightarrow{(x,y) \mapsto y-x} H_*(C_{i+1}^{\text{id}}) = N_{\text{id},i+1} = N_{(i+1),i+1}. \end{aligned}$$

Such diamonds are called *transposition diamonds*, and it has been shown in [MO15, Theorem 2.4] that the morphism induced by σ_{vine}^i between the lower and upper parts of the diamond matches bars with same representative positive chains together. Hence, bars in $\mathcal{B}(N_{\text{id}})$ and $\mathcal{B}(N_{(i+1)})$, and thus the bars in $\mathcal{B}(\mathbb{M}|_{l_1})$ and $\mathcal{B}(\mathbb{M}|_{l_2})$ are matched under σ_{vine} are associated to the same summand of \mathbb{M} , and thus are compatible. In particular, when \mathbb{M} is decomposable into intervals summands, σ_{vine} is exact. Finally, by repeating this argumentation with the other transpositions induced by the simplices reordering from l_i to l_{i+1} , for $i = 2, \dots, k-1$ one has that the same is true for bars in $\mathcal{B}(\mathbb{M}|_l)$ and $\mathcal{B}(\mathbb{M}|_{l'})$. \square

6 Numerical experiments

In this section, we showcase the performances of **MMA**. More precisely, we empirically study how the output quality and running time depend on the precision δ and the number of lines $|L|$. Then, we compare the running times of **MMA** with those of **Rivet** [LW15] and the elder-rule staircode (ERS) [CKMW20]. Finally, we investigate how running time is affected by the number of filtrations. All experiments were done on a laptop with AMD Ryzen 4800 CPU and 16GB of RAM. Our code is publicly available at <https://github.com/DavidLapous/multipers>.

Data sets and filtrations. In our first two experiments, we focus on two real-world data sets of point clouds. The first ones, called **LargeHypoxicRegion**, were obtained from immunohistochemistry in [Vip20b]. These are made of a few thousand points, each representing a single cell. The others were obtained from applying time-delay embedding in \mathbb{R}^2 on time series taken from a few data sets (**Wine**, **Plane**, **OliveOil**, **Coffee**) from the UCR archive [Che15]. On all of these data sets, we computed bi-filtrations using the standard Vietoris-Rips filtration, and the superlevel sets of a Gaussian kernel density estimation (with bandwidth parameter $0.1d$ where d is the diameter of the dataset), and we applied **MMA** and its competitors on the corresponding multi-parameter persistence modules in homology dimensions 0 and 1 (note that the ERS can only compute dimension 0).

In our third experiment, we measure the dependence on the number of filtrations using a synthetic data set obtained by sampling 300 points in the unit square $[0, 1]^2$, computing their Alpha simplicial complex, and generating n random filtration values on the points.

Finally, it is worth noting that we used multi-parameter edge collapses [AKP22] in order to simplify the multi-parameter persistence modules (without losing information) as much as possible before applying **Rivet** and **MMA**. The timing of this simplifications are not taken into account, but they are not the computational bottleneck of our computations. Furthermore, for the **LargeHypoxicRegion**, we thresholded the Rips edges at 0.02, leading to simplicial complexes of $\sim 85k$ and $\sim 125k$ simplices respectively, after simplifications.

Convergence of MMA. We first empirically validate Propositions 3.4 and 4.13 by measuring how far is the output of **MMA** from the data when the precision parameter δ decreases and the number of lines in L increases. For this, we used the bottleneck distances between the fibered barcodes (on 100 random diagonal lines) of the outputs of **MMA** and the ones of the underlying modules as a proxy for the interleaving distances (since they are practically very difficult to evaluate). We call this the *estimated matching distance*. Results are displayed in Figure 13. One can see that the convergence is empirically linear with the number of lines $|L|$,

which is in line with Propositions 3.4 and 4.13 (since $|L|$ increases linearly as δ decreases for a fixed n). Note that the distance even reaches 0 on a few cases.

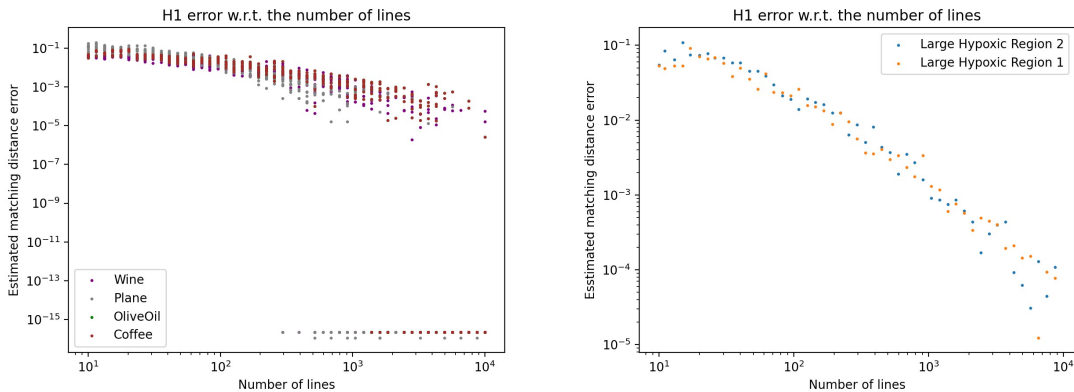


Figure 13: Convergence on UCR data sets (left) and immunohistochemistry data sets (right).

Running times. We now compare the running times of `MMA` with those of `Rivet` and the ERS. Results can be found in Table 1. It is worth noting that on several occasions, `Rivet` and the ERS could not produce outputs in reasonable time, due (among other things) to large memory consumption. On the other hands, the fact that `MMA` produces discretely presented intervals allows to encode them in a sparse manner with their corners. Note that computations with `Rivet` can be also approximated by coarsening the filtration values, and thus the module. In practice, this corresponds to restricting the 2-module to a $\kappa = \kappa_x \times \kappa_y$ grid, where $\kappa_x, \kappa_y \in \mathbb{N}$ are the resolutions in both axes, see [LW15, Section 8.2]. The parameters κ and $|L|$ have (roughly) the same role, and can be related with $\sqrt{\kappa} \simeq |L|$ (for a given, prescribed precision). Overall, we find that the running times of `MMA` outperforms its competitors, except when κ is very small. However, in this case, the corresponding output of `Rivet` is very crude as the module is restricted on just a few points, whereas `MMA` produces intervals that are accurate along whole straight lines: we find that for large data sets, `MMA` is the only method that can produce accurate representations.

	Rivet			ERS	MMA		
	$\kappa = 10^2$	$\kappa = 50^2$	$\kappa = 100^2$		$ L = 100$	$ L = 1000$	$ L = 10,000$
Coffee	$0.21 \pm 0.01, 0.18 \pm 0.01$	$9.75 \pm 5.92, 0.35 \pm 0.12$	$-, 0.95 \pm 0.56$	0.34 ± 0.04	0.0093 ± 0.001	0.024 ± 0.001	0.16 ± 0.008
Plane	$0.19 \pm 0.005, 0.18 \pm 0.03$	$4.36 \pm 2.24, 0.28 \pm 0.04$	$33.3 \pm 17.5, 0.56 \pm 0.17$	0.09 ± 0.03	0.004 ± 0.0	0.012 ± 0.001	0.095 ± 0.004
Wine	$0.21 \pm 0.003, 0.19 \pm 0.007$	$8.50 \pm 2.00, 0.22 \pm 0.01$	$-, 0.28 \pm 0.023$	0.22 ± 0.04	0.004 ± 0.0	0.016 ± 0.0	0.129 ± 0.002
OliveOil	$0.21 \pm 0.004, 0.19 \pm 0.002$	$5.55 \pm 1.20, 0.31 \pm 0.016$	$-, 0.82 \pm 0.17$	1.39 ± 0.03	0.026 ± 0.001	0.058 ± 0.001	0.37 ± 0.006
Worms	$0.29 \pm 0.082, 0.23 \pm 0.23$	$19.9 \pm 14.4, 4.60 \pm 5.0$	$-, 31.36 \pm 36.24$	3.85 ± 0.1	0.22 ± 0.11	0.34 ± 0.15	1.35 ± 0.41
LargeHypoxicRegion1	1.73, 2.88	--, 234	--, --	--	26.4	26.6	59.4
LargeHypoxicRegion2	2.39, 6.04	--, --	--, --	--	57.3	54.3	102.9

Table 1: Mean and variances of the running times (s) for `Rivet`, the ERS and `MMA`. We provide both degree 0 (left) and 1 (right) homology timings for `Rivet`, whereas the timings of `MMA` include both. The double dashes correspond to out of memory errors, i.e., a memory usage that is over 12GB.

Interestingly, computing 0-dimensional homology is sometimes slower than 1-dimensional homology for `Rivet`; as it relies on computing minimal free presentations, we think that this comes from the fact that minimal presentations in homology dimension 0 can be more complex than their counterparts in homology dimension 1, i.e., they have much more generators. We also investigate how running times of `MMA` depend on the number of lines. Unsurprisingly, one can see from Figure 14 that running time increases with the number of lines. However, the dependency looks empirically sublinear, which could come from the fact that even though there are more lines, these lines are closer to each other, and thus matching them with vineyards

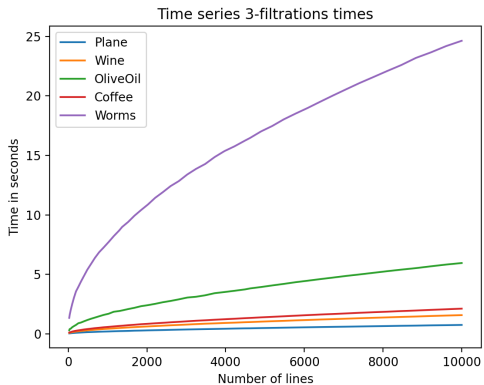


Figure 14: Running time (s) needed to run MMA on the UCR datasets.

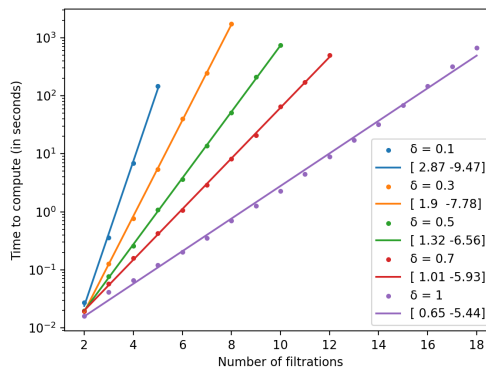


Figure 15: Running time (s) of MMA w.r.t. the number n of filtrations.

requires fewer computation steps. This is also highlighted by the running times of `LargeHypoxicRegion2`, Table 1 which are smaller when computing it over 1 000 lines than 100 lines.

Dependence on number of filtrations. Finally, we investigate how the running times of MMA depend on the number n of filtrations. While most of the approaches in the literature are limited to $n = 2$ parameters, one can see from Figure 15 that MMA can produce outputs in a reasonable amount of time for up to $n \simeq 10$ parameter filtrations. As expected from the complexity of MMA in Equation 8, the running times increase exponentially with n .

7 Conclusion

In this article, we presented MMA: a new scheme for computing topological invariants (in the form of candidate decompositions) of multi-parameter persistence modules, in a fast and robust way, and whose complexity, running time, and approximation error can be controlled by user-defined parameters. We then showcased the performances of our method on synthetic and real data sets. Our code is publicly available at <https://github.com/DavidLapous/multipers>.

There are a number of interesting directions for future work.

1. We conjecture that the family of candidate decompositions produced by varying matching functions completely recovers multi-dimensional persistence modules.
2. We proved that our candidate has bounded approximation error when approximating interval decomposable modules. We also proved stability even when the underlying module is not interval decomposable. Is there some kind of optimality result describing the relationship of the candidate decomposition to the underlying module in this case?
3. Recently, stability results have become available for specific multi-parameter persistence modules [BL20]. We expect that these can be used to infer theoretical confidence regions and convergence rates for our candidate decompositions.

References

- [ABE⁺18] Hideto Asashiba, Mickaël Buchet, Emerson Escolar, Ken Nakashima, and Michio Yoshiwaki. On interval decomposability of 2D persistence modules. In *CoRR*. arXiv:1812.05261, 2018.

- [AEK⁺17] Henry Adams, Tegan Emerson, Michael Kirby, Rachel Neville, Chris Peterson, Patrick Shipman, Sofya Chepushtanova, Eric Hanson, Francis Motta, and Lori Ziegelmeier. Persistence images: a stable vector representation of persistent homology. *Journal of Machine Learning Research*, 18(8):1–35, 2017.
- [AENY19] Hideto Asashiba, Emerson Escobar, Ken Nakashima, and Michio Yoshiwaki. On approximation of 2D persistence modules by interval-decomposables. In *CoRR*. arXiv:1911.01637, 2019.
- [AKP22] Ángel Javier Alonso, Michael Kerber, and Siddharth Pritam. Filtration-domination in bifiltered graphs. In *CoRR*. arXiv:2211.05574, 2022.
- [BHO18] Mickaël Buchet, Yasuaki Hiraoka, and Ipepei Obayashi. Persistent homology and materials informatics. In *Nanoinformatics*, pages 75–95. Springer-Verlag, 2018.
- [BL18] Magnus Botnan and Michael Lesnick. Algebraic stability of zigzag persistence modules. *Algebraic and Geometric Topology*, 18(6):3133–3204, 2018.
- [BL20] Andrew Blumberg and Michael Lesnick. Stability of 2-parameter persistent homology. In *CoRR*. arXiv:2010.09628, 2020.
- [BL22] Magnus Botnan and Michael Lesnick. An introduction to multiparameter persistence. In *CoRR*. arXiv:2203.14289, 2022.
- [BLO22] Magnus Botnan, Vadim Lebovici, and Steve Oudot. On rectangle-decomposable 2-parameter persistence modules. *Discrete & Computational Geometry*, 2022.
- [BLOr] Magnus Botnan, Vadim Lebovici, and Steve Oudot. Local characterizations for decomposability of 2-parameter persistence modules. In *CoRR*. arXiv:2008.02345, 2020. To appear in *Algebras and Representation Theory*.
- [BOO21] Magnus Botnan, Steffen Oppermann, and Steve Oudot. Signed barcodes for multi-parameter persistence via rank decompositions and rank-exact resolutions. In *CoRR*. arXiv:2107.06800, 2021.
- [Bub15] Peter Bubenik. Statistical topological data analysis using persistence landscapes. *Journal of Machine Learning Research*, 16(3):77–102, 2015.
- [Car09] Gunnar Carlsson. Topology and data. *Bulletin of the American Mathematical Society*, 46(2):255–308, 2009.
- [CB20] Mathieu Carrière and Andrew Blumberg. Multiparameter persistence image for topological machine learning. In *Advances in Neural Information Processing Systems 34 (NeurIPS 2020)*, pages 22432–22444. Curran Associates, Inc., 2020.
- [CCI⁺20] Mathieu Carrière, Frédéric Chazal, Yuichi Ike, Théo Lacombe, Martin Royer, and Yuhei Umeda. PersLay: a neural network layer for persistence diagrams and new graph topological signatures. In *23rd International Conference on Artificial Intelligence and Statistics (AISTATS 2020)*, pages 2786–2796. PMLR, 2020.
- [CCO17] Mathieu Carrière, Marco Cuturi, and Steve Oudot. Sliced Wasserstein kernel for persistence diagrams. In *34th International Conference on Machine Learning (ICML 2017)*, volume 70, pages 664–673. PMLR, 2017.
- [CdSGO16] Frédéric Chazal, Vin de Silva, Marc Glisse, and Steve Oudot. *The structure and stability of persistence modules*. SpringerBriefs in Mathematics. Springer-Verlag, 2016.
- [Che15] Chen, Yanping and Keogh, Eamonn and Hu, Bing and Begum, Nurjahan and Bagnall, Anthony and Mueen, Abdullah and Batista, Gustavo. The UCR time series classification archive, 2015.

- [CKMW20] Chen Cai, Woojin Kim, Facundo Mémoli, and Yusu Wang. Elder-rule-staircodes for augmented metric spaces. In *36th International Symposium on Computational Geometry (SoCG 2020)*, pages 26:1–26:17. Schloss Dagstuhl–Leibniz-Zentrum fuer Informatik, 2020.
- [CO19] Jérémy Cochoy and Steve Oudot. Decomposition of exact pfd persistence bimodules. *Discrete & Computational Geometry*, pages 1–39, 2019.
- [CSEM06] David Cohen-Steiner, Herbert Edelsbrunner, and Dmitriy Morozov. Vines and vineyards by updating persistence in linear time. In *22nd Annual Symposium on Computational Geometry (SoCG 2006)*, pages 119–126. Association for Computing Machinery, 2006.
- [DKM22] Tamal Dey, Woojin Kim, and Facundo Mémoli. Computing generalized rank invariant for 2-parameter persistence modules via zigzag persistence and its applications. In *38th International Symposium on Computational Geometry (SoCG 2022)*, volume 224, pages 34:1–34:17. Schloss Dagstuhl–Leibniz-Zentrum für Informatik, 2022.
- [dMV11] Vin de Silva, Dmitriy Morozov, and Mikael Vejdemo-Johansson. Dualities in persistent (co)homology. *Inverse Problems*, 27(12):124003, 2011.
- [DW22] Tamal Dey and Yusu Wang. *Computational topology for data analysis*. Cambridge University Press, 2022.
- [DX21] Tamal Dey and Cheng Xin. Rectangular approximation and stability of 2-parameter persistence modules. In *CoRR*. arXiv:2108.07429, 2021.
- [DX22] Tamal Dey and Cheng Xin. Generalized persistence algorithm for decomposing multiparameter persistence modules. *Journal of Applied and Computational Topology*, 2022.
- [EH10] Herbert Edelsbrunner and John Harer. *Computational topology: an introduction*. American Mathematical Society, 2010.
- [KM18] Woojin Kim and Facundo Mémoli. Generalized persistence diagrams for persistence modules over posets. In *CoRR*. arXiv:1810.11517, 2018.
- [KR21] Michael Kerber and Alexander Rolle. Fast minimal presentations of bi-graded persistence modules. In *Symposium on Algorithm Engineering and Experiments (ALENEX 2021)*, pages 207–220, 2021.
- [Lan18] Claudia Landi. The rank invariant stability via interleavings. In *Research in Computational Topology*, pages 1–10. Springer, 2018.
- [Les15] Michael Lesnick. The theory of the interleaving distance on multidimensional persistence modules. *Foundations of Computational Mathematics*, 15(3):613–650, 2015.
- [LW15] Michael Lesnick and Matthew Wright. Interactive visualization of 2D persistence modules. In *CoRR*. arXiv:1512.00180, 2015.
- [LW19] Michael Lesnick and Matthew Wright. Computing minimal presentations and bigraded Betti numbers of 2-parameter persistent homology. In *CoRR*. arXiv:1902.05708, 2019.
- [MO15] Clément Maria and Steve Oudot. Zigzag persistence via reflections and transpositions. In *26th Annual ACM-SIAM Symposium on Discrete Algorithms (SODA 2015)*, pages 181–199. Society for Industrial and Applied Mathematics, 2015.
- [Mun84] James Munkres. *Elements of algebraic topology*. CRC Press, 1984.
- [Oud15] Steve Oudot. *Persistence theory: from quiver representations to data analysis*, volume 209 of *Mathematical Surveys and Monographs*. American Mathematical Society, 2015.

- [RB19] Raúl Rabadán and Andrew Blumberg. *Topological data analysis for genomics and evolution*. Cambridge University Press, 2019.
- [RHBK15] Jan Reininghaus, Stefan Huber, Ulrich Bauer, and Roland Kwitt. A stable multi-scale kernel for topological machine learning. In *28th IEEE Conference on Computer Vision and Pattern Recognition (CVPR 2015)*, pages 4741–4748. IEEE Computer Society, 2015.
- [Vip20a] Oliver Vipond. Local equivalence of metrics for multiparameter persistence modules. In *CoRR*. arXiv:2004.11926, 2020.
- [Vip20b] Oliver Vipond. Multiparameter persistence landscapes. *Journal of Machine Learning Research*, 21(61):1–38, 2020.